AE3-401 Advanced Mechanics of Flight

Part II - Atmospheric Flight Dynamics

Rafael Palacios
Department of Aeronautics
Imperial College London

October 26, 2019

Contents

Chapter 1

Rigid-Aircraft Equations of Motion

1.1 Kinematics of rigid aircraft

1.1.1 Frames of reference

In this chapter, the aircraft will be considered as a rigid body whose position and orientation, as a function of time, will be expressed with respect to an observer in a certain *inertial frame of reference* (FoR). A frame fixed to a point in the Earth does not actually define an inertial FoR, since, in general, Earth kinematics has a non-negligible effect on typical flight paths in the atmosphere. In this course, we will assume however the "flat Earth" assumption, which approximates as inertial a FoR fixed to the Earth's surface. Furthermore, in that frame gravity will be assumed to be a constant vertical force which is independent of the altitude.

The orientation of the aircraft with respect to that inertial frame will be defined by a *body-fixed frame of reference*, rigidly-linked to the aircraft and with origin at its center of mass (CM) . Most aircraft have a plane of symmetry, and it is customary to define the body-fixed axes such that the y axis is normal to the symmetry plane and positive on the starboard (right) wing. In that case y becomes a principal axis of inertia. Two possible definitions could be considered then for the x axis:

- *Principal axes.* The x axis is also selected as a principal axis of inertia. This simplifies the inertia tensor (see next section), which becomes diagonal, but will complicate the equations of motion, as this principal axis would normally be tilted downwards with respect to the aircraft velocity vector.

- *Stability axes.* The x axis corresponds to the forward flight direction of the aircraft in some nominal conditions. Note that its definition will therefore change with the point in the flight envelope (as, for example, the aircraft may fly at different angles

of incidence). Also, since the axes are body-attached, the instantaneous aircraft velocity vector will not necessarily be along the x axis during manoeuvres.

Most derivations in this course will be done using the vehicle's stability axes. However, an additional set of axes, referred to as the *wind axes*, is sometimes also useful. It is defined such that x is always tangent to the flight path and positive forward, and z is in the plane of symmetry and positive downward. Note that wind axes are *not* a body-fixed FoR.

1.1.2 Euler angles

The orientation between two FoR and, in particular, between the Earth and the body-fixed frames, will be parametrised using Euler angles. They are defined by three successive rotations, starting from the Earth frame, defined as in Figure 1.1,

1. A rotation Ψ about the vertical direction z_E of the Earth frame. Ψ is the vehicle *heading* (or yaw). The resulting frame after the rotation will be called 1.

2. A rotation Θ about the horizontal direction y_1. Θ is the vehicle *pitch* and the new frame is called 2.

3. A rotation Φ about the longitudinal direction x_2. Φ is the vehicle *bank* (or roll) and the final frame defines the body-fixed stability axis.

Once the order and the range of the rotations is defined, the three Euler angles that define the relative orientation between two frames of reference are unique. The convention above (yaw first, pitch second, roll third, also known as 3-2-1), and shown in detail in fig. 1.2, is the one typically used in classic flight dynamics.Those Euler angles allow now the transformation of coordinates of vectors in 3-D space: We will express the FoR in which the components are given by a subindex, so, e.g., $\mathbf{V}_E$ is the velocity vector expressed in its components in the Earth frame. In the body frame it will be $\mathbf{V}_B = \mathbf{T}_{BE}\mathbf{V}_E$, with $\mathbf{T}_{BE}$ the coordinate transformation matrix between both frames, which is obtained as

$$\mathbf{T}_{BE} = \begin{bmatrix} 1 & 0 & 0 \\ 0 & \cos\Phi & \sin\Phi \\ 0 & -\sin\Phi & \cos\Phi \end{bmatrix} \begin{bmatrix} \cos\Theta & 0 & -\sin\Theta \\ 0 & 1 & 0 \\ \sin\Theta & 0 & \cos\Theta \end{bmatrix} \begin{bmatrix} \cos\Psi & \sin\Psi & 0 \\ -\sin\Psi & \cos\Psi & 0 \\ 0 & 0 & 1 \end{bmatrix} \tag{1.1}$$

We write it in shorthand form as $\mathbf{T}_{BE} = \boldsymbol{\tau}_x(\Phi)\boldsymbol{\tau}_y(\Theta)\boldsymbol{\tau}_z(\Psi)$. The coordinate transformation matrix from body to Earth can be now obtained simply by reversing the order

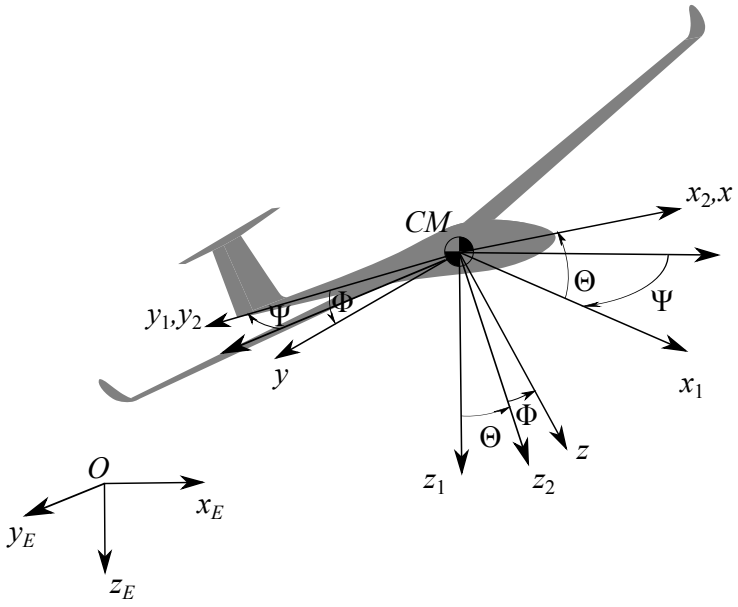

Figure 1.1: Euler angles between Earth and body-fixed FoR.

of the rotations, that is, first a rotation about x, then a about y and then about z with angles equal an opposite to those defined above. Noting that each rotation is a matrix multiplication, they appear right to left in the expression as

$$\mathbf{T}_{EB} = \mathbf{T}_{BE}^{-1} = \mathbf{T}_{BE}^{\top} = \boldsymbol{\tau}_z(-\Psi)\boldsymbol{\tau}_y(-\Theta)\boldsymbol{\tau}_x(-\Phi). \tag{1.2}$$

Introduce quatern

1.1.3 Angular velocity

Consider now an arbitrary point P in a rigid body that has a rotational motion around its CM. Its position vector with respect to the body's CM, and expressed in its components in the body-fixed FoR, will be

$$\mathbf{r}_B^{(P)} = \begin{Bmatrix} x \\ y \\ z \end{Bmatrix}, \tag{1.3}$$

which, since the body is rigid, will be constant with time. Its inertial velocity is defined then as

$$\mathbf{V}_E^{(P)} = \mathbf{V}_E + \dot{\mathbf{r}}_E^{(P)} = \mathbf{V}_E + \dot{\mathbf{T}}_{EB}\mathbf{r}_B^{(P)}, \tag{1.4}$$

where $\mathbf{V}_E$ is the velocity vector of the CM defined in section 1.1.2 above. In terms of its components in the body-fixed frame, and noting that it is $\mathbf{V}_E = \mathbf{T}_{EB}\mathbf{V}_B$, the velocity of

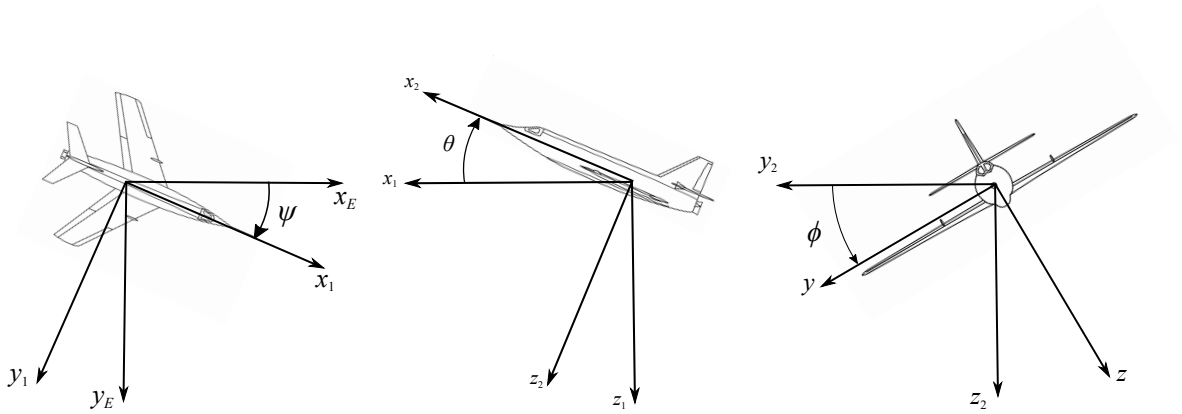

(a) First rotation: Yaw (b) Second rotation: Pitch (c) Third rotation: Roll

Figure 1.2: The three successive rotations defining local aircraft orientation.

P will be given as

$$\mathbf{V}_B^{(P)} = \mathbf{V}_B + \mathbf{T}_{BE}\dot{\mathbf{T}}_{EB}\mathbf{r}_B^{(P)}. \tag{1.5}$$

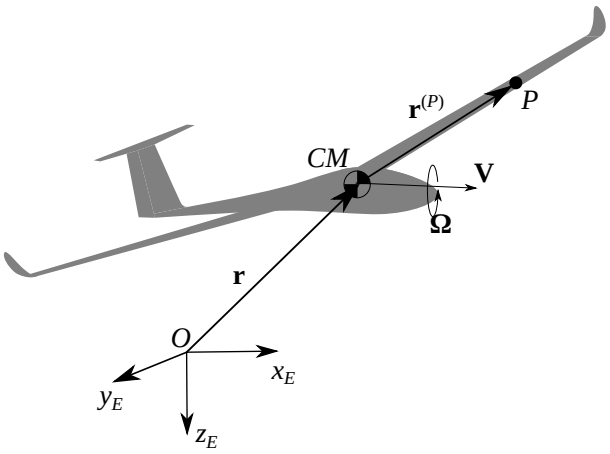

Figure 1.3: Kinematic description of a rigid aircraft.

We will identify the components of the velocity vector, in the body-fixed FoR, as $\mathbf{V}_B = \begin{Bmatrix} V_x & V_y & V_z \end{Bmatrix}^\top$. From the properties (1.2), it is $\mathbf{T}_{BE}\mathbf{T}_{EB} = \mathbf{1}$, a unit matrix. Therefore, it is $\frac{d}{dt}(\mathbf{T}_{BE}\mathbf{T}_{EB}) = \mathbf{0}$. We also have

$$\frac{d}{dt}(\mathbf{T}_{BE}\mathbf{T}_{EB}) = \mathbf{T}_{BE}\dot{\mathbf{T}}_{EB} + \dot{\mathbf{T}}_{BE}\mathbf{T}_{EB} = \mathbf{T}_{BE}\dot{\mathbf{T}}_{EB} + \left(\mathbf{T}_{EB}^\top\dot{\mathbf{T}}_{BE}^\top\right)^\top, \tag{1.6}$$

and therefore

$$\mathbf{T}_{BE}\dot{\mathbf{T}}_{EB} + \left(\mathbf{T}_{BE}\dot{\mathbf{T}}_{EB}\right)^\top = \mathbf{0}. \tag{1.7}$$

This means that $\mathbf{T}_{BE}\dot{\mathbf{T}}_{EB}$ is a skew-symmetric matrix. It is well known that a skew-symmetric matrix only have three independent coefficients, which we will define as the three components of the instantaneous *angular velocity* of the body, $\boldsymbol{\Omega}_B$

$$\mathbf{T}_{BE}\dot{\mathbf{T}}_{EB} = \begin{bmatrix} 0 & -\Omega_z & \Omega_y \\ \Omega_z & 0 & -\Omega_x \\ -\Omega_y & \Omega_x & 0 \end{bmatrix} = \tilde{\boldsymbol{\Omega}}_B. \tag{1.8}$$

We will refer to the operator $(\tilde{\bullet})$ as the *cross-product operator*, since Eq. (1.5) can now be written as

$$\mathbf{V}_B^{(P)} = \mathbf{V}_B + \tilde{\boldsymbol{\Omega}}_B \mathbf{r}_B^{(P)} = \mathbf{V}_B + \boldsymbol{\Omega}_B \times \mathbf{r}_B^{(P)}. \tag{1.9}$$

Finally, we can write the angular velocity from the time derivative of the Euler angles by combining Eqs. (1.8) and (1.1). The algebra is rather tedious, but it is also rather straightforward. After going through it, the inertial angular velocity, expressed in its components in the body-fixed FoR, can be shown to be[1]

$$\boldsymbol{\Omega}_B = \begin{Bmatrix} \Omega_x \\ \Omega_y \\ \Omega_z \end{Bmatrix} = \begin{Bmatrix} \dot{\Phi} \\ 0 \\ 0 \end{Bmatrix} + \boldsymbol{\tau}_x(\Phi) \begin{Bmatrix} 0 \\ \dot{\Theta} \\ 0 \end{Bmatrix} + \boldsymbol{\tau}_x(\Phi)\boldsymbol{\tau}_y(\Theta) \begin{Bmatrix} 0 \\ 0 \\ \dot{\Psi} \end{Bmatrix}. \tag{1.10}$$

Note that this equation can also be obtained by superposition of three angular velocities defined by the rate of change of the Euler angles around their respective axes of rotation. This occurs because angular velocities are vector quantities. Eq. (1.10) finally results in

$$\boldsymbol{\Omega}_B = \begin{bmatrix} 1 & 0 & -\sin\Theta \\ 0 & \cos\Phi & \sin\Phi\cos\Theta \\ 0 & -\sin\Phi & \cos\Phi\cos\Theta \end{bmatrix} \begin{Bmatrix} \dot{\Phi} \\ \dot{\Theta} \\ \dot{\Psi} \end{Bmatrix}. \tag{1.11}$$

1.2 Flight dynamics equations

1.2.1 Inertia characteristics

Each particle P in the vehicle, whose position vector is $\mathbf{r}_B^{(P)}$ as defined in Eq. (1.3), can be associated to an infinitesimal mass dm. If $\mathcal{V}$ is the volume of the aircraft, the total mass of the vehicle is $m = \int_{\mathcal{V}} dm$. By the definition of the CM, it is also $\int_{\mathcal{V}} \mathbf{r}_B^{(P)} dm = \mathbf{0}$. The aircraft CM moves with a certain inertial linear and angular velocity, $\mathbf{V}_B$ and $\boldsymbol{\Omega}_B$,

[1] Most textbooks define the components of the angular velocity in stability axes as $\boldsymbol{\Omega}_B = \begin{Bmatrix} P & Q & R \end{Bmatrix}^\top$.

respectively. We define the associated total *translational (or linear) momentum*, $\mathbf{P}_B$, as

$$\begin{aligned}\mathbf{P}_B &= \int_{\mathcal{V}} \mathbf{V}_B^{(P)} dm = \int_{\mathcal{V}} \left(\mathbf{V}_B + \boldsymbol{\Omega}_B \times \mathbf{r}_B^{(P)} \right) dm \\ &= \mathbf{V}_B \int_{\mathcal{V}} dm + \boldsymbol{\Omega}_B \times \int_{\mathcal{V}} \mathbf{r}_B^{(P)} dm = m\mathbf{V}_B,\end{aligned} \tag{1.12}$$

and the total *angular momentum*, about the CM, $\mathbf{H}_B$, as

$$\begin{aligned}\mathbf{H}_B &= \int_{\mathcal{V}} \mathbf{r}_B^{(P)} \times \mathbf{V}_B^{(P)} dm \\ &= \int_{\mathcal{V}} \mathbf{r}_B^{(P)} \times \left(\mathbf{V}_B + \boldsymbol{\Omega}_B \times \mathbf{r}_B^{(P)} \right) dm \\ &= -\mathbf{V}_B \times \int_{\mathcal{V}} \mathbf{r}_B^{(P)} dm - \int_{\mathcal{V}} \mathbf{r}_B^{(P)} \times (\mathbf{r}_B^{(P)} \times \boldsymbol{\Omega}_B) dm = \mathbf{I}_B \boldsymbol{\Omega}_B,\end{aligned} \tag{1.13}$$

where the first term is zero from the definition of $\mathbf{r}_B^{(P)}$, and the second term defines the *inertia tensor* in the body-fixed axes, $\mathbf{I}_B$, which can be written as

$$\mathbf{I}_B = \begin{bmatrix} I_{xx} & -I_{xy} & -I_{xz} \\ -I_{yx} & I_{yy} & -I_{yz} \\ -I_{zx} & -I_{zy} & I_{zz} \end{bmatrix}. \tag{1.14}$$

The terms in the diagonal are the moments of inertia of the body. It is, e.g., $I_{xx} = \int_{\mathcal{V}} (y^2 + z^2) dm$. The non-diagonal terms depend on the products of inertia, e.g., $I_{yz} = I_{zy} = \int_{\mathcal{V}} yz dm$. When the aircraft is symmetric about the y axis, it is $I_{xy} = 0$ and $I_{yz} = 0$.

If expressed in its components in the Earth frame, the angular momentum becomes

$$\mathbf{H}_E = \mathbf{T}_{EB} \mathbf{H}_B = \mathbf{T}_{EB} \mathbf{I}_B \mathbf{T}_{BE} \boldsymbol{\Omega}_E. \tag{1.15}$$

Since, by definition is $\mathbf{H}_E = \mathbf{I}_E \boldsymbol{\Omega}_E$, the coordinate transformation on the inertia tensor is then $\mathbf{I}_E = \mathbf{T}_{EB} \mathbf{I}_B \mathbf{T}_{BE}$. Assuming that the mass distribution of the rigid aircraft does not change with time, both mass m and inertia $\mathbf{I}_B$ are constant magnitudes, while $\mathbf{I}_E$ depends on the aircraft orientation.

1.2.2 Equations of motion for a rigid body

The equations of motion (EoM) are obtained from Newton's second law, applied to a rigid-body under external forces. Recall that Newton's equations in vector form are written in inertial components. Since, the aircraft is subject to time-dependent external forces, the force resultant (the sum of all the external forces on the aircraft) will be written as $\mathbf{F}_E(t)$ and the moment resultant, about the CM, will be $\mathbf{M}_E(t)$. As a result,

the EoM will be

$$\begin{aligned} \frac{d\mathbf{P}_E}{dt} &= \frac{d}{dt}\left(m\mathbf{V}_E\right) = \mathbf{F}_E \\ \frac{d\mathbf{H}_E}{dt} &= \frac{d}{dt}\left(\mathbf{I}_E\boldsymbol{\Omega}_E\right) = \mathbf{M}_E \end{aligned} \tag{1.16}$$

As it was just mentioned, in the Earth frame the inertia tensor, $\mathbf{I}_E$, will be a function of time. Therefore, it is more convenient to write the equations in stability axis. In particular, since it is $\mathbf{H}_E = \mathbf{T}_{EB}\mathbf{H}_B$, it is $\dot{\mathbf{H}})_E = \dot{\mathbf{T}}_{EB}\mathbf{H}_B + \mathbf{T}_{EB}\dot{\mathbf{H}}_B$. Using this relation, and the transformations above, we finally obtain

$$\begin{aligned} m\dot{\mathbf{V}}_B + m\boldsymbol{\Omega}_B \times \mathbf{V}_B &= \mathbf{F}_B^{(aero)} + \mathbf{F}_B^{(prop)} + \mathbf{F}_B^{(grav)} \\ \mathbf{I}_B\dot{\boldsymbol{\Omega}}_B + \boldsymbol{\Omega}_B \times \mathbf{I}_B\boldsymbol{\Omega}_B &= \mathbf{M}_B^{(aero)} + \mathbf{M}_B^{(prop)} \end{aligned} \tag{1.17}$$

where the external forces have been split between aerodynamic, thrust and gravitational forces. Those are discussed next.

1.2.3 Gravitational forces

For a given aircraft mass, m, and under the flat Earth assumptions, the gravitational forces in body-fixed axis will depend on the orientation of the vehicle. Noting that the z axis in the Earth frame is positive down, the resultant force (at the CM) is

$$\mathbf{F}_B^{(grav)} = \mathbf{T}_{BE}m\mathbf{g} = \mathbf{T}_{BE}\begin{Bmatrix} 0 \\ 0 \\ mg \end{Bmatrix}. \tag{1.18}$$

In terms of the Euler angles introduced in Eq. (1.1), it is

$$\mathbf{F}_B^{(grav)} = \begin{Bmatrix} -mg\sin\Theta \\ mg\cos\Theta\sin\Phi \\ mg\cos\Theta\cos\Phi \end{Bmatrix}. \tag{1.19}$$

Therefore, the gravitational forces introduce an explicit dependency on the vehicle orientation in the EoM[2]. That means that we have to solve simultaneously Eqs. (1.17), which determine the six components of the linear and angular velocities, and Eq. (1.8), which links the Euler angles and the angular velocity. Inversion of this equation gives the

[2]A second potential dependency on the absolute spatial orientation occurs when the aircraft flies through thermal columns in the atmosphere.

differential equations that determine the aircraft orientation as a function of time. It is

$$\begin{Bmatrix} \dot{\Phi} \\ \dot{\Theta} \\ \dot{\Psi} \end{Bmatrix} = \begin{bmatrix} 1 & \sin\Phi\tan\Theta & \cos\Phi\tan\Theta \\ 0 & \cos\Phi & -\sin\Phi \\ 0 & \sin\Phi\sec\Theta & \cos\Phi\sec\Theta \end{bmatrix} \begin{Bmatrix} \Omega_x \\ \Omega_y \\ \Omega_z \end{Bmatrix}. \tag{1.20}$$

1.2.4 Propulsive forces

The propulsion system generates a thrust force, T, on the vehicle. Thrust is typically[3] expressed in terms of a nondimensional *thrust coefficient*, C_T, which is assumed to be a known function of the airspeed, V_∞, and a throttle setting, δ_T. It is defined as

$$T = \tfrac{1}{2}\rho_\infty V_\infty^2 S C_T(V_\infty, \delta_T) \tag{1.21}$$

where ρ_∞ is the local density. In powerplant selection, S is either the propeller disk area or the engine exhaust area, but in flight dynamics modelling it is the main wing reference area. For a given mass configuration of the aircraft, the instantaneous thrust will generate a resultant force and moment at the CM, which will depend on the position and orientation of the propulsive devices in the stability axes. Assuming that the propulsion system is symmetric with respect to the aircraft x-z plane, the geometric parameters become the coordinates x_T and z_T, as well as the pitch orientation θ_T, as shown in Figure 1.4. That finally defines the propulsive forces in Eq. (1.17) as,

$$\mathbf{F}_B^{(prop)} = \begin{Bmatrix} T\cos\theta_T \\ 0 \\ -T\sin\theta_T \end{Bmatrix}, \text{ and } \mathbf{M}_B^{(prop)} = \begin{Bmatrix} 0 \\ T(z_T\cos\theta_T + x_T\sin\theta_T) \\ 0 \end{Bmatrix}. \tag{1.22}$$

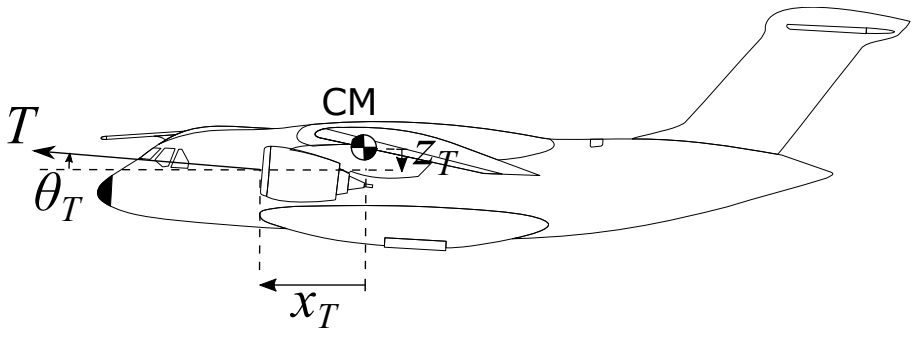

Figure 1.4: Propulsion system geometry definition.

[3]See section 2.5 of Stengel (2004) for details on typical powerplants.

1.2.5 Aerodynamic forces

The aerodynamic forces will, in general, have non-zero resultants on all three components of the force and moment equations (1.17). We will assume that the time scales in the aircraft manoeuvres are large enough such that quasi-steady aerodynamics can be considered, although their specific description may vary quite substantially depending on the flight conditions and the characteristics of the vehicle. In general, we can state that they will depend on (Ashley, 1974):

- Vehicle geometry (magnitudes such as, wingspan, typical chord c, reference wing area S, aerofoil shape, etc.).
- Air density, Mach and Reynolds number in the flight condition.
- Instantaneous relative linear and angular velocity between the vehicle and the atmosphere, and its time derivatives.
- Deflection of the control surfaces (typically elevators, δ_e; ailerons, δ_a, and rudder, δ_r) and its time derivatives.

This can be written as

$$\begin{aligned} \mathbf{F}_{aB} &= \tfrac{1}{2}\rho_\infty V_\infty^2 S_{ref} \mathbf{c}_{\mathbf{F}_B}\left(\mathbf{V}_B, \boldsymbol{\Omega}_B, \boldsymbol{\delta}_c; \mathrm{Ma}, \mathrm{Re}\right), \\ \mathbf{M}_{aB} &= \tfrac{1}{2}\rho_\infty V_\infty^2 S_{ref} \boldsymbol{\Lambda}_{ref} \mathbf{c}_{\mathbf{M}_B}\left(\mathbf{V}_B, \boldsymbol{\Omega}_B, \boldsymbol{\delta}_c; \mathrm{Ma}, \mathrm{Re}\right), \end{aligned} \tag{1.23}$$

where $\boldsymbol{\delta}_c(t)$ is the vector with the instantaneous deflection angles in each of the control surfaces, Ma and Re are the Mach and Reynolds number at the nominal conditions, $\boldsymbol{\Lambda}_{ref} = \mathrm{diag}\left(b_{ref}, c_{ref}, b_{ref}\right)$, and $\mathbf{c}_{\mathbf{F}_B}$ and $\mathbf{c}_{\mathbf{M}_B}$ are the non-dimensional forces and moments after normalizing with the dynamic pressure, a reference area S_{ref}, and reference lengths c_{ref} and b_{ref}. Typically, those are chosen as S_{ref} is the planform wing area, c_{ref} is the mean aerodynamic chord of the wing and b_{ref} is the wing span. The subindex B is retained in both force and moment coefficients to indicate that their three components correspond to a projection on stability axes. We will define specific aerodynamic models for each of the configurations studied in this course.

1.3 State and input vectors

From a mathematical point of view, we will then see the aircraft as a dynamical system for which we will be concerned about its equilibrium conditions (trimmed flight, static manoeuvres), stability (its ability to return to the equilibrium when it is perturbed), and

manoeuvrability (response to commanded inputs). For that, we define the *state vector* for the rigid-aircraft dynamics, $\mathbf{x}_r$, as

$$\mathbf{x}_r = \begin{Bmatrix} V_x & V_y & V_z & \Omega_x & \Omega_y & \Omega_z & \Phi & \Theta \end{Bmatrix}^\top, \tag{1.24}$$

and the *input vector*, $\mathbf{u}$, as

$$\mathbf{u} = \begin{Bmatrix} \delta_e & \delta_a & \delta_r & \delta_T \end{Bmatrix}^\top. \tag{1.25}$$

The state vector includes all the necessary information to track future vehicle kinematics given its current values and the future time-histories of the inputs. We have not included the heading, Ψ, as this value has no effect in the vehicle dynamics – we say that the dynamics are *invariant* with respect to Ψ. With this, we can write the dynamics of the system, given by Eqs. (1.17) and (1.20), in their most generic form, as

$$\begin{aligned} \dot{\mathbf{x}}_r &= \mathbf{f}(\mathbf{x}_r, \mathbf{u}) \\ &= \mathbf{f}_{gyr}(\mathbf{x}_r) + \mathbf{f}_{aero}(\mathbf{x}_r, \mathbf{u}) + \mathbf{f}_{prop}(\mathbf{x}_r, \mathbf{u}) + \mathbf{f}_{grav}(\mathbf{x}_r). \end{aligned} \tag{1.26}$$

The term $\mathbf{f}_{gyr}$ represents the gyroscopic forces defined by the cross-products with the angular velocity in Eq. (1.17). The initial conditions are typically given by the aircraft in equilibrium, that is, a set of inputs, $\mathbf{u}(0) = \mathbf{u}_0$, and states, $\mathbf{x}_r(0) = \mathbf{x}_{r0}$, for which it is $\mathbf{f}(\mathbf{x}_{r0}, \mathbf{u}_0) = \mathbf{0}$. Eq. (1.26) is normally complemented by an output equation, that extracts magnitudes of interest (for instance, to interface with a flight simulator). In its most general form, they are written as,

$$\mathbf{y} = \mathbf{g}(\mathbf{x}_r, \mathbf{u}), \tag{1.27}$$

where $\mathbf{y}$ is a generic *output vector*. This will often be a linear combination of the states (usually the values of certain states themselves), but it could also include magnitudes defined by nonlinear relations, such as the instantaneous absolute velocity, $V = \sqrt{V_x^2 + V_y^2 + V_z^2}$. The flow diagram describing Eqs. (1.26) and (1.27) is the simple input/output (I/O) relation shown in Figure 1.5.

Figure 1.5: Basic block diagram for the aircraft state equations.

1.4 Further reading

Most books in flight mechanics have detailed derivations of the rigid-aircraft equations of motion. Here we followed closely that of Ashley (1974).

Chapter 2

Small-perturbation dynamics

2.1 Steady climb

Consider now a trimmed aircraft following a rectilinear flight path with constant velocity V_∞, levelled wings ($\Phi_0 = 0$), and inclined at an angle Θ_0 above the horizontal. This reference situation defines the simplest steady manoeuvre, which will be discussed in some detail the next chapter. The equations of motion will be written in the stability axes for this configuration, which are shown in Figure 2.1. We assume that the aircraft is symmetric about the xz-plane, which implies that $I_{xy} = 0$ and $I_{yz} = 0$ in the inertia tensor (1.14). If the thrust, T_0, goes along the x axis (that is, $\theta_T = 0$ and $z_T = 0$ in Eq. (1.22)), then the aerodynamic forces at this reference condition will be such that

$$\begin{aligned} L_0 &= mg\cos\Theta_0, \\ D_0 &= T_0 - mg\sin\Theta_0. \end{aligned} \tag{2.1}$$

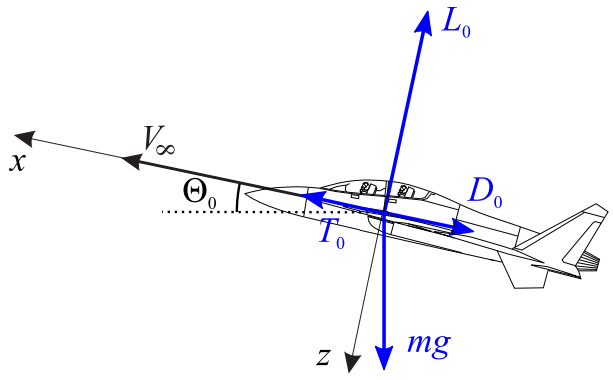

Figure 2.1: Reference conditions: steady climb.

The resultant aerodynamic moments at the CM are also zero in the reference condition. We are interested in the small perturbations to this reference trajectory, that is, we consider the case

$$\begin{aligned} V_x &= V_\infty + v_x, & \Omega_x &= \omega_x, & \Phi &= \phi, \\ V_y &= v_y, & \Omega_y &= \omega_y, & \Theta &= \Theta_0 + \theta, \\ V_z &= v_z, & \Omega_z &= \omega_z, \end{aligned} \tag{2.2}$$

where lowercase refers to small magnitudes. The equations of motion are described by the linearization of the EoM (1.17) around this reference point.

$$\begin{aligned} m\dot{v}_x &= \Delta F_x - (mg\cos\Theta_0)\,\theta, \\ m\dot{v}_y &= \Delta F_y + (mg\cos\Theta_0)\,\phi - mV_\infty\omega_z, \\ m\dot{v}_z &= \Delta F_z - (mg\sin\Theta_0)\,\theta + mV_\infty\omega_y, \\ I_{xx}\dot{\omega}_x - I_{xz}\dot{\omega}_z &= \Delta M_x, \\ I_{yy}\dot{\omega}_y &= \Delta M_y, \\ -I_{xz}\dot{\omega}_x + I_{zz}\dot{\omega}_z &= \Delta M_z, \\ \dot{\phi} &= \omega_x + \omega_z\tan\Theta_0, \\ \dot{\theta} &= \omega_y. \end{aligned} \tag{2.3}$$

Angles $\Theta_0 + \theta$ and ϕ are the instantaneous climb and bank flight-path angles, respectively. The azimuth angle, ψ, does not affect the dynamics and has not been included. Note also that we have used the trigonometric relations

$$\begin{aligned} \sin\Theta &= \sin(\Theta_0+\theta) = \sin\Theta_0\cos\theta + \sin\theta\cos\Theta_0 \approx \sin\Theta_0 + \theta\cos\Theta_0, \\ \cos\Theta &= \cos(\Theta_0+\theta) = \cos\Theta_0\cos\theta - \sin\Theta_0\sin\theta \approx \cos\Theta_0 - \theta\sin\Theta_0. \end{aligned} \tag{2.4}$$

2.2 Longitudinal problem under constant-thrust assumption

The incremental forces ΔF_x and ΔF_z are the tangent and normal forces on the body-fixed frame after perturbations. We will assume that thrust is constant (and always aligned with the x axis), although in reality the thrust is affected by changes in aircraft speed and attitutde. In this case, ΔF_x and ΔF_z will only depend on the aerodynamic forces. Noting that v_z is positive down, the instantaneous incremental angle of attack is defined as

$$\Delta\alpha = \tan^{-1}\left(\frac{v_z}{V_\infty + v_x}\right) \approx \frac{v_z}{V_\infty}. \tag{2.5}$$

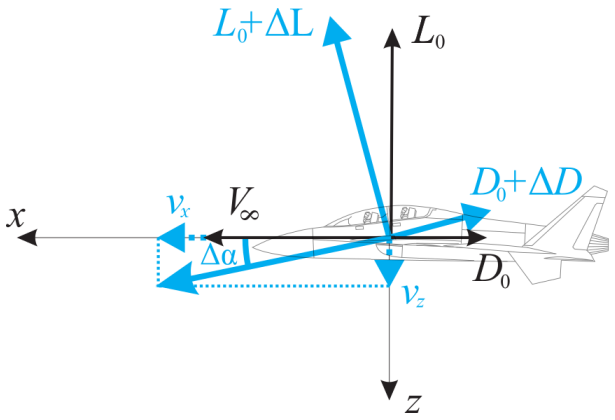

Figure 2.2: Aerodynamic forces in the small-perturbation longitudinal problem

Recall that a positive angle of attack corresponds to a positive vertical component of the velocity in the incoming flow, or to a negative velocity of the aircraft with respect to the flow, as it is the case here. This is in addition to the constant angle of attack that generates the lift L_0 in the reference condition, Eq. (2.1), as shown in Figure 2.2. By definition, lift will be always normal to the instantaneous velocity vector, and as a result, the incremental forces become

$$\begin{aligned}
\Delta F_x &= (L_0 + \Delta L)\sin\Delta\alpha - (D_0 + \Delta D)\cos\Delta\alpha - (-D_0) \\
&\approx L_0\Delta\alpha - \Delta D, \\
\Delta F_z &= -(L_0 + \Delta L)\cos\Delta\alpha - (D_0 + \Delta D)\sin\Delta\alpha - (-L_0) \\
&\approx -\Delta L - D_0\Delta\alpha.
\end{aligned} \tag{2.6}$$

where L_0 and D_0 are the reference aerodynamic forces, which can be replaced by Eq. (2.1), and ΔL and ΔD are those that appear due to v_x and v_z. It will be

$$\begin{aligned}
L = L_0 + \Delta L &= \frac{1}{2}\rho_\infty (V_\infty + v_x)^2 S(C_{L0} + \Delta C_L) \\
&\approx L_0 + \rho_\infty V_\infty v_x S C_{L0} + \frac{1}{2}\rho_\infty V_\infty^2 S\Delta C_L,
\end{aligned} \tag{2.7}$$

and finally

$$\Delta L \approx 2L_0\frac{v_x}{V_\infty} + \frac{1}{2}\rho_\infty V_\infty^2 S\Delta C_L = \frac{2v_x}{V_\infty}mg\cos\Theta_0 + \frac{1}{2}\rho_\infty V_\infty^2 S\Delta C_L. \tag{2.8}$$

Similarly, we obtain that the incremental drag is

$$\Delta D \approx \frac{2v_x}{V_\infty}\left(T_0 - mg\sin\Theta_0\right) + \frac{1}{2}\rho_\infty V_\infty^2 S\Delta C_D. \tag{2.9}$$

Defining the reference dynamic pressure as $q_\infty = \frac{1}{2}\rho_\infty V_\infty^2$, the incremental forces and moments are then written as

$$\begin{aligned}
\Delta F_x &= \left(mg\cos\Theta_0\right)\frac{v_z}{V_\infty} - q_\infty S\Delta C_D - 2\left(T_0 - mg\sin\Theta_0\right)\frac{v_x}{V_\infty},\\
\Delta F_z &= -2\left(mg\cos\Theta_0\right)\frac{v_x}{V_\infty} - q_\infty S\Delta C_L - \left(T_0 - mg\sin\Theta_0\right)\frac{v_z}{V_\infty},\\
\Delta M_y &= q_\infty Sc\Delta C_{M_y},
\end{aligned} \tag{2.10}$$

where S and c are the main wing area and mean aerodynamic chord. All the aircraft-level aerodynamic coefficients are defined using S and c as normalization constants.

Quasi-steady aerodynamic model

The lift coefficient will be obtained next under a quasi-steady approximation. Let $C_{L\alpha}^w$ and $C_{L\alpha}^t$ be the lift curve slope of the wing and horizontal tail, respectively, and let $C_{L\delta}^t$ be the tail lift increment to unit elevator input, then we have

$$\Delta C_L = \Delta C_L^w + \Delta C_L^t = C_{L\alpha}\frac{\Delta v_z}{V_\infty} + \frac{S_t}{S}\left(C_{L\alpha}^t\frac{l_t\Delta\omega_y}{V_\infty} + C_{L\delta}^t\delta_e\right), \tag{2.11}$$

where $C_{L\alpha} = C_{L\alpha}^w + \frac{S_t}{S}C_{L\alpha}^t$ and l_t is the distance between the CM and the aerodynamic centre of the tail. Note that the lift coefficients at the tail are normalized with the gross tail area, S_t. They also include the effect of the downwash of the main wing. We have assumed however that the tail lift is in the same direction as in the main wing, which neglects the contributions of the wing downwash and the pitch rotation, ω_y, to the instantaneous wind velocity vector on the tail. At subsonic speeds, the drag coefficient is assumed constant with the forward flight velocity, but will depend on the lift coefficient (and hence the angle of attack) through the induced drag. That is,

$$C_D = C_{D0} + \frac{S}{\pi b^2 e}C_L^2, \tag{2.12}$$

where the efficiency factor is $e = 0.8$ for a rectangular wing. Assuming that e and the aspect ratio take the same value at both wing and tail, it is

$$\Delta C_D = \frac{2S}{\pi b^2 e}C_L\Delta C_L \approx \frac{2SC_{L0}C_{L\alpha}}{\pi b^2 e}\frac{v_z}{V_\infty}. \tag{2.13}$$

In the last expression, we have assumed the lift increments by only the first (the dominant) term in Eq. (2.11). Finally, the pitch moment coefficient (positive nose up) will be approximated by the contributions of the lift on wing and tail, as

$$\begin{aligned}\Delta C_{M_y} &= \frac{l_w}{c}\Delta C_L^w - \frac{l_t}{c}\Delta C_L^t \\ &= \left(\frac{l_w}{c}C_{L\alpha}^w - \frac{S_t l_t}{Sc}C_{L\alpha}^t\right)\frac{v_z}{V_\infty} - \frac{S_t l_t}{Sc}C_{L\alpha}^t\frac{\omega_y l_t}{V_\infty} - \frac{S_t l_t}{Sc}C_{L\delta}^t\delta_e,\end{aligned} \tag{2.14}$$

where l_w is the distance between the CM and the aerodynamic centre of the wing (positive if the wing is ahead of the CM).

State equation

Substituting all the previous expressions into Eq. (2.3), one has finally the linear EoM for the small-perturbation longitudinal vehicle dynamics, as

$$\begin{aligned}m\dot{v}_x =& mg\cos\Theta_0\left(1 - \frac{2SC_{L\alpha}}{\pi b^2 e}\right)\frac{v_z}{V_\infty} - 2\left(T_0 - mg\sin\Theta_0\right)\frac{v_x}{V_\infty} \\ &- mg\cos\Theta_0\theta, \\ m\dot{v}_z =& -2mg\cos\Theta_0\frac{v_x}{V_\infty} - \left[q_\infty SC_{L\alpha} + \left(T_0 - mg\sin\Theta_0\right)\right]\frac{v_z}{V_\infty} \\ &- q_\infty S_t\left[C_{L\alpha}^t\frac{\omega_y l_t}{V_\infty} + C_{L\delta}^t\delta_e\right] - mg\sin\Theta_0\theta + mV_\infty\omega_y, \\ I_{yy}\dot{\omega}_y =& q_\infty Sc\left[\frac{l_w}{c}C_{L\alpha}^w - \frac{S_t l_t}{Sc}C_{L\alpha}^t\right]\frac{v_z}{V_\infty} - q_\infty S_t l_t\left[C_{L\alpha}^t\frac{\omega_y l_t}{V_\infty} + C_{L\delta}^t\delta_e\right], \\ \dot{\theta} =& \omega_y.\end{aligned} \tag{2.15}$$

The state vector in this problem will be $\mathbf{x}_r = \begin{Bmatrix} v_x & v_z & \omega_y & \theta \end{Bmatrix}^\top$ and the corresponding linear state equations are

$$\dot{\mathbf{x}}_r = \mathbf{A}_r\mathbf{x}_r + \mathbf{B}_r\delta_e, \tag{2.16}$$

with the constant-coefficient *state matrix*

$$\mathbf{A}_r = \begin{bmatrix} \frac{2(mg\sin\Theta_0 - T_0)}{mV_\infty} & \frac{g\cos\Theta_0}{V_\infty}\left(1 - \frac{2SC_{L\alpha}}{\pi b^2 e}\right) & 0 & -g\cos\Theta_0 \\ -\frac{2g\cos\Theta_0}{V_\infty} & \frac{mg\sin\Theta_0 - T_0}{mV_\infty} - \frac{\rho_\infty V_\infty SC_{L\alpha}}{2m} & V_\infty - \frac{\rho_\infty V_\infty S_t l_t C_{L\alpha}^t}{2m} & -g\sin\Theta_0 \\ 0 & \frac{\rho_\infty V_\infty\left(Sl_w C_{L\alpha}^w - S_t l_t C_{L\alpha}^t\right)}{2I_{yy}} & -\frac{\rho_\infty V_\infty S_t l_t^2 C_{L\alpha}^t}{2I_{yy}} & 0 \\ 0 & 0 & 1 & 0 \end{bmatrix}, \tag{2.17}$$

and the *input matrix*, which in this case is a column matrix,

$$\mathbf{B}_r = \begin{bmatrix} 0 & -\frac{q_\infty S_t C^t_{L\delta}}{m} & -\frac{q_\infty S_t l_t C^t_{L\delta}}{I_{yy}} & 0 \end{bmatrix}^\top . \tag{2.18}$$

The eigenvalues of the state matrix determine the dynamic response characteristics of the aircraft. They are typically two complex pairs: a low-frequency low-damping pair, known as the long-period (or phugoid) mode, and a higher-frequency higher-damping pair, known as the short-period mode. Both are schematically shown in the complex plane in fig. 2.3, including their typical dependencies with the vehicle centre of mass (which enters the equations through l_w and l_t), and the horizontal tail area, S_t, with all other parameters in Equation (2.17) being constant.

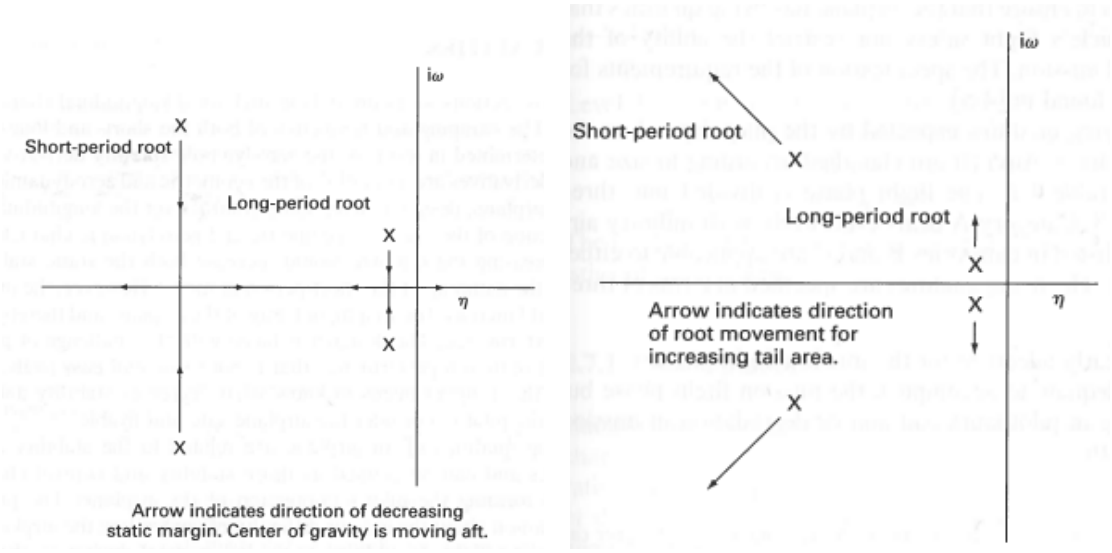

(a) Effect of centre of gravity position (b) Effect of horizontal tail area

Figure 2.3: Typical longitudinal eigenvalues with key dependencies (Nelson, 1998).

In chapter 5.3 we will define an autopilot based on *full-state feedback*. Consequently, we assume that there are appropriate sensors on the vehicle to measure the instantaneous velocities of all states $\mathbf{x}_r$. The output equation is then the identity relation

$$\mathbf{y}_r = \mathbf{C}_r \mathbf{x}_r, \tag{2.19}$$

with

$$\mathbf{C}_r = \begin{bmatrix} 1 & 0 & 0 & 0 \\ 0 & 1 & 0 & 0 \\ 0 & 0 & 1 & 0 \\ 0 & 0 & 0 & 1 \end{bmatrix} \tag{2.20}$$

Chapter 3

Commanded Manoeuvres

In these lectures we are concerned with the *maneuverability* of fixed-wing aircraft, that is, their ability to follow a desired flight path, and on the *manoeuvre loads*, that is, the internal stresses that appear in the vehicle structure –due to the change of external forces necessary to alter the vehicle trajectory–. In general, we differentiate between *steady* and *dynamic manoeuvres* depending on whether the aircraft velocity components in the body-attached reference frame are constant with time or time-dependent. In the first part, section 3.1, we will consider steady manoeuvres, which are used to define the nominal manoeuvring envelope of a given vehicle. Then in section 3.2 we will discuss some dynamic manoeuvres, first from an energy point of view and then as an optimal control problem

3.1 Steady Manoeuvres

Equilibrium (or steady) manoeuvres correspond to solutions of (1.17) with constant translational and angular velocity in the body-attached reference frame, that is

$$\begin{aligned} \mathbf{F}_B^{(aero)} + \mathbf{F}_B^{(prop)} + \mathbf{F}_B^{(grav)} - m\boldsymbol{\Omega}_B \times \mathbf{V}_B = 0, \\ \mathbf{M}_B^{(aero)} + \mathbf{M}_B^{(prop)} - \boldsymbol{\Omega}_B \times \mathbf{I}_B\boldsymbol{\Omega}_B = 0, \end{aligned} \tag{3.1}$$

which are solved together with the kinematic relations defined by eq. (1.20). The typical equilibrium manoeuvres considered in vehicle design are steady climb, steady pull-out and steady turn, which are shown schematically in Figure 3.1. In a *steady climb* the aircraft follows a rectilinear trajectory at constant speed, that is the non-zero terms in the state vector are $V_x = V$ and $\Theta = \Theta_0$, which are both constant with time. The

resulting equilibrium conditions are

$$\begin{aligned} L - mg\cos\Theta_0 &= 0, \\ T - D - mg\sin\Theta_0 &= 0. \end{aligned} \tag{3.2}$$

The characteristics of the climb are closely linked to the available thrust. The metric used for this is the *specific excess power*, which will be discussed in section 3.2.

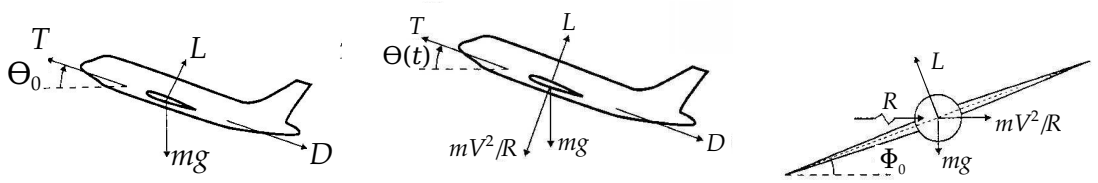

(a) Steady climb (b) Steady pull-out (c) Steady turn

Figure 3.1: Equilibrium manoeuvres (Wright and Cooper, 2007).

In steady pull-out and turn manoeuvres, the aircraft follows a circular trajectory in either a vertical (pull-out) or a horizontal (turn) plane. Let R be the radius of the trajectory in either case. The corresponding centripetal forces have been included in the free-body diagrams of figs. 3.1b and 3.1c. In the case of *steady pull-out*, it will be $V_x = V$ and $\Omega_y = \frac{V}{R}$, both constant. Since, it is $\Omega_y = \dot{\Theta}$, the pitch angle will vary with time, as $\Theta(t) = \Theta_0 + \frac{V}{R}t$. The equilibrium equations in this case are

$$\begin{aligned} L - mg\cos\Theta(t) - m\frac{V^2}{R} &= 0, \\ T - D - mg\sin\Theta(t) &= 0, \end{aligned} \tag{3.3}$$

This clearly requires that lift (and therefore drag) and thrust are constantly updated to sustain the manoeuvre. Finally, the *steady turn* is similarly defined with constant rate $\frac{V}{R}$ and constant roll angle Φ_0. As stability axis are body fixed, this defines an angular velocity with two non-zero components $\Omega_y = -\frac{V}{R}\sin\Phi_0$ and $\Omega_z = -\frac{V}{R}\cos\Phi_0$. Translational velocity is still $V_x = V$ and equilibrium in stability axes, Equation (3.1), leads to

$$\begin{aligned} T - D &= 0, \\ mg\sin\Phi_0 - m\frac{V^2}{R}\cos\Phi_0 &= 0, \\ mg\cos\Phi_0 - L + m\frac{V^2}{R}\sin\Phi_0 &= 0. \end{aligned} \tag{3.4}$$

The equilibrium equations in a steady turn are however more naturally written in vertical and horizontal axes, as

$$\begin{aligned} L\cos\Phi_0 - mg &= 0, \\ L\sin\Phi_0 - m\frac{V^2}{R} &= 0. \end{aligned} \tag{3.5}$$

Needless to say, Equation (3.5) is obtained directly from Equation (3.5). Steady turn is therefore achieved with a fixed commanded input on the vehicle controls. Euler angles are $\Phi(t) = \Phi_0$, $\Theta(t) = 0$, and $\Psi = \Psi_0 + \frac{V}{R}t$, where Ψ_0 is the initial heading at $t = 0$. Note finally, the components of the angular velocity satisfy Equation (1.10).

For a given aircraft, its manoeuvrability characteristics in pull-out and turn (in particular, the achievable turning radius R) will be closely linked to the available lift. The metric used here is the *load factor*, which is discussed next.

3.1.1 Load factor and manoeuvring envelope

We define the *load factor*, n, as the ratio between the instantaneous lift and the aircraft weight, that is, $n = \frac{L}{mg}$. Manoeuvres are normally defined by their load factor and the maximum manoeuvring load factor that a vehicle can sustain is a key structural sizing parameter. It ranges from values as low as 2 or 3, in the case of transport aircraft, to values as high as 8 or 9, for fighter planes. It is however customary to "measure" load factors with respect to gravity, so one would talk about a "$6g$" manoeuvre. For the three conditions shown in figure 3.1, it is easy to show that the load factors are

$$\begin{aligned} n_{climb} &= \cos\Theta_0, \\ n_{pull-out} &= \cos\Theta + \frac{V^2}{gR}, \\ n_{turn} &= \frac{1}{\cos\Phi_0}. \end{aligned} \tag{3.6}$$

Note that $n_{pull-out}$ is only defined as an instantaneous load factor, as the pitch orientation of the aircraft will vary during the manoeuvre. In fact, pull-out manoeuvres for airframe design are defined on level flight conditions, $\Theta = 0$, since this defines the maximum value of $n_{pull-out}$. Commercial transport aircraft regulations require the airframe to be able to sustain a $2.5g$ pull-out from level flight. At the opposite extreme, a very small, or even zero, load factor can be obtained if the aircraft performs this manoeuvre with a negative angular velocity. This is the situation for parabolic flights, which generate the perception of weightlessness inside the cabin.

The maximum and minimum load factors that an aircraft can sustain (for given gross

weight, configuration –e.g., clean or landing–, and altitude) will depend on the airspeed. This defines the vehicle's *manoeuvring envelope* (or V-n diagram). A typical diagram is shown in Figure 3.2: The upper and lower limits in the load factor (n_{max} and n_{min}) are the structural limits; the minimum and maximum speed are operational speeds at the chosen altitude (stall and dive velocity, respectively). At the lower speeds, the maximum and minimum achievable load factor are determined by stall conditions (C_{Lmax} and C_{Lmin}, respectively).

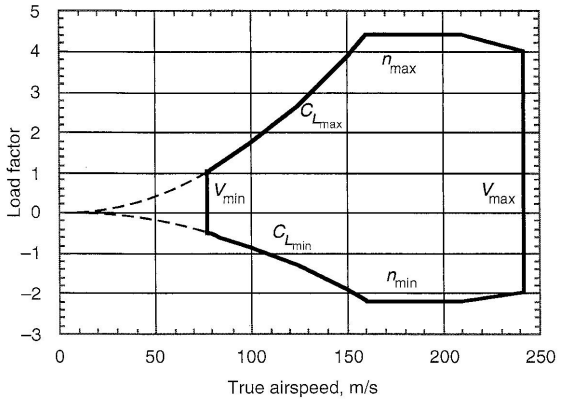

Figure 3.2: Typical manoeuvring envelope (Stengel, 2004).

The smallest speed at which the aircraft can achieve maximum load factor is the so-called *corner velocity*, V_{co}. At this speed one obtains the minimum turn radius, R_{min}, (and the maximum attainable turn rate) at the given altitude and configuration. The minimum turn radius is derived from Eq. (3.5), that is,

$$\begin{aligned} L\cos\Phi_{max} &= mg, \\ L\sin\Phi_{max} &= \frac{mV_{co}^2}{R_{min}}, \end{aligned} \tag{3.7}$$

where the maximum roll angle is obtained from the maximum load factor in (3.6), that is, $\cos\Phi_{max} = 1/n_{max}$. As a result, it is

$$\begin{aligned} \frac{mV_{co}^2}{R_{min}} &= \frac{mg}{\cos\Phi_{max}}\sin\Phi_{max} \\ &= mg\frac{\sqrt{1-\cos^2\Phi_{max}}}{\cos\Phi_{max}} \\ &= mg\sqrt{n_{max}^2-1}, \end{aligned} \tag{3.8}$$

and, finally,

$$R_{min} = \frac{V_{co}^2}{g\sqrt{n_{max}^2 - 1}}. \tag{3.9}$$

Note that the previous results assume that we have enough thrust and lift available to keep altitude and airspeed during the turning manoeuvre at maximum load factor.

Manoeuvre Load Alleviation

The design of large air vehicles nowadays typically considers *manoeuvre load alleviation* (MLA) systems, which use a distribution of flaps along the span such that each manoeuvre is achieved by the combination that provides the smallest loading on the wing structure. In a pull-out that implies minimizing the root moments on the wings for a desired increase of lift, which naturally implies using flaps and ailerons as closed to the fuselage as possible. Figure 3.3 shows a typical MLA set-up during aircraft take-off. MLA for more complex (dynamic) manoeuvres imply feedback controllers that minimize a cost function that include key wing load variables.

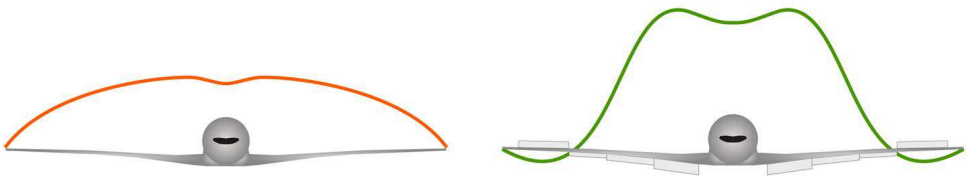

(a) Clean configuration (b) Take-off configuration

Figure 3.3: Take-off configuration with load alleviation (Xu and Kroo, 2014).

3.2 Dynamic manoeuvres

In the previous section we have seen that steady manoeuvres are mostly associated with the availability of additional lift (measured by the load factor) from the aerodynamic surfaces. The implicit assumption was that there is also enough thrust available to sustain the manoeuvre, although this is strictly not necessary if the manoeuvre has a short duration. In general, however, the aircraft may also accelerate or decelerate as part of the manoeuvre, in which case we refer to it as dynamic. Investigating them requires solution to the equations of motions, but some important information on *aircraft performance* can be obtained from simple energy analysis.

3.2.1 Energy methods: Specific excess power

The total energy of an aircraft flying at altitude h with airspeed V is $\mathcal{E} = \frac{1}{2}mV^2 + mgh$, that is, the sum of its kinetic and potential energy. The energy normalized by the aircraft weight is referred to as the *specific energy* (or energy height), h_e, that is,

$$h_e = \frac{\mathcal{E}}{mg} = \frac{V^2}{2g} + h. \tag{3.10}$$

An aircraft can exchange kinetic by potential energy quite efficiently as part of a manoeuvre. For that it is useful to plot the contour lines of constant specific energy in the vehicle flight envelope, defined by flight altitude and Mach number, as shown in fig. 3.4.

To consider changes of specific energy we will assume that the aircraft moves along a rectilinear climb trajectory in the vertical plane with flight path angle γ and that the thrust force vector is always aligned with the velocity vector. Its acceleration along the trajectory will be

$$m\dot{V} = T - D - mg\sin\gamma, \tag{3.11}$$

and its rate of climb will be

$$\dot{h} = V\sin\gamma. \tag{3.12}$$

If we now differentiate Eq. (3.10) with time and substitute Eqs. (3.11) and (3.12), we have,

$$\begin{aligned} \dot{h}_e &= \frac{V}{g}\dot{V} + \dot{h} = \frac{V(T-D)}{mg} + V\sin\gamma - V\sin\gamma \\ &= \frac{V(T-D)}{mg}. \end{aligned} \tag{3.13}$$

This magnitude is know as the *specific excess power*, $P_s = \frac{V(T-D)}{mg}$, and determines authority of the vehicle engines to gain specific energy (and more specifically, altitude). Noting that the induced drag grows quadratically with the lift, which implies that $D = K_0 + K_1L^2$, we have that the drag in Eq. (3.13) will depend quadratically on the load factor, $D = K_0 + K_1(nmg)^2$. For a given engine, the maximum available thrust will depend on the velocity and altitude. As a result, for a given aircraft configuration the specific excess power will be a function of the load factor, the flight velocity, and the altitude, $P_s = P_s(V, n, h)$.

Minimum time to climb

For a given load factor, Figure 3.4 shows the contour lines of constant P_s as we change flight velocity and altitude on a certain aircraft. The figure also includes the contour lines of constant specific energy, h_e, given by Eq. (3.10), that is $h = h_e - \frac{V^2}{2g}$. This will allow us to establish some maneouvrability characteristics of the aircraft. Consider first the time need to move between two values of specific energy. This may correspond to a climb/descent, a increase/decrease in speed, or any combination of them. Since it is $\dot{h}_e = P_s$, it will be

$$t_2 - t_1 = \int_{h_{e_1}}^{h_{e_2}} \frac{\mathrm{d}h_e}{P_s}. \tag{3.14}$$

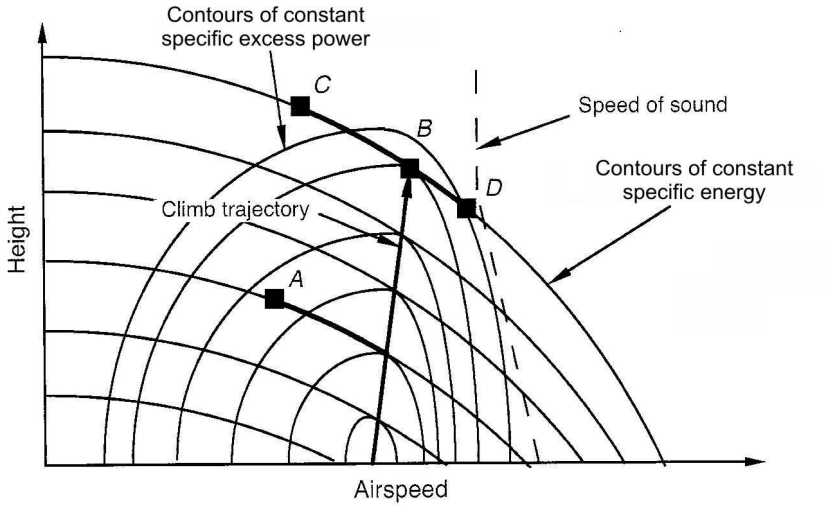

Figure 3.4: Typical minimum-time climb path in subsonic flight (Stengel, 2004).

The *minimum time to climb* will be obtained if at each altitude the aircraft is at its point of maximum specific power. That defines the line marked with an arrow in Figure 3.4 (note that it does not need to be a straight line, but it is typically not far from for it). The minimum-time path between A and either C or D, would be then normally achieved as follows:

1. An acceleration along the constant specific energy line until the maximum P_s line. This implies an exchange altitude by speed, which is normally refered to as *zoom dive*.

2. A climb along the maximum P_s line until point B.

3. Either a zoom dive to point D, or a zoom climb to point C, depending on our target flight point.

This trajectory in the altitude/velocity plot is shown in Figure 3.4. Finally, if we replace time with fuel, we obtain the *minimum-fuel-to-climb trajectory*. For that we first need to know the specific fuel consumption of the aircraft, which is given as the ratio between the mass flow rate of propellant and the thrust. Most commercial flights use minimum-fuel climb and descent paths.

3.2.2 Optimal control methods

Energy methods are very useful at the design phase, mainly to size aircraft propulsion to achieve a baseline performance. Once the features of the aircraft has been established, trajectory planning and control design have traditionally used the more rigorous framework provided by *optimal control* theory.

The optimal control problem is to determine the "best" set of control actions $\mathbf{u}(t)$ that can be picked to achieve a preset control objective, which is mathematically defined by means of a metric of performance. Optimal control theory is concerned with establishing those best-performing control signals that will minimize (or maximize) that performance criterion while meeting any physical constraints that may exist in the system. Optimal control can be applied to linear or nonlinear systems, with time-invariant or time-dependent dynamics, and with various levels of complexity in the definitions of the problem constraints. To introduce the problem we will restrict ourselves to *linear* optimal control problems, which seek a control signal $\mathbf{u}(t)$ that causes a dynamical system

$$\dot{\mathbf{x}} = \mathbf{A}\mathbf{x} + \mathbf{B}\mathbf{u} \tag{3.15}$$

to have a response $\mathbf{x}$ (known as *trajectory* in the state space) that minmises a *cost function* $J = J(\mathbf{x}(t), \mathbf{u}(t), t)$ in an interval $0 \leq t \leq t$, with initial conditions $\mathbf{x}(0) = \mathbf{x}_0$. This defines a constrained minimization problem, that is, the minimisation of the cost function subject to constraints on state and control (in particular, that they satisfy the initial conditions at $t = 0$ and the equations of motion for $0 \leq t \leq t_f$). Mathematically, we write this problem as

$$\begin{aligned} \min_{\mathbf{x},\mathbf{u}} \quad & J\left(\mathbf{x}(t), \mathbf{u}(t), t\right) \\ \text{subject to} \quad & \mathbf{A}\mathbf{x} + \mathbf{B}\mathbf{u} - \dot{\mathbf{x}} = \mathbf{0} \quad \text{for all} \quad t \in [0, t_f] \\ & \mathbf{x}(0) = \mathbf{x}_0 \end{aligned} \tag{3.16}$$

Most optimal control problems need to be solved under certain contraints on the values

that either the inputs or states, or both, can take, but this is not be considered here. Typical optimal control problems are:

Minimum-time problems. They minimize the time in the transfer between two states, that is,

$$J = t_f - t_0 = \int_{t_0}^{t_f} \mathrm{d}t \tag{3.17}$$

Terminal-control problems. They minimise the deviation of the state at time t_f from a reference $\bar{\mathbf{x}}_f$. For simplicity of notation, we also define $\mathbf{x}_f = \mathbf{x}(t_f)$. The usual cost function is

$$J = \left(\mathbf{x}_f - \bar{\mathbf{x}}_f\right)^\top \mathbf{H} \left(\mathbf{x}_f - \bar{\mathbf{x}}_f\right) \tag{3.18}$$

with $\mathbf{H}$ a real symmetric positive definitive weighting matrix.

Minimum-control effort problems. The objective is now to minimum the control effort to achieve a certain goal. The usual cost function is

$$J = \int_0^{t_f} \mathbf{u}^\top \mathbf{R}\mathbf{u}\, \mathrm{d}t \tag{3.19}$$

with $\mathbf{R}$ a real symmetric positive definitive weighting matrix.

Regulator problems. This is a combination of the last two with zero reference, that is,

$$J(\mathbf{x}(t), \mathbf{u}(t)) = \frac{1}{2}\mathbf{x}_f^\top \mathbf{H}\mathbf{x}_f + \frac{1}{2}\int_0^{t_f} \left[\mathbf{x}^\top \mathbf{Q}\mathbf{x} + \mathbf{u}^\top \mathbf{R}\mathbf{u}\right] \mathrm{d}t. \tag{3.20}$$

The cost (3.20) has three symmetric weighting matrices: $\mathbf{R}$ is positive definite, and $\mathbf{Q}$ and $\mathbf{H}$ are positive semidefinite. The first term in the equation is the terminal cost, which penalizes any deviations from zero on the state at the end of the time interval. The first term inside the integral penalizes non-zero values of the system states during the interval. Therefore, the relative magnitude between $\mathbf{H}$ and $\mathbf{Q}$ determines whether we are concerned about keeping the reference trajectory (which is zero in this case) at all times or achieving a certain state at t_f. Finally, the second term in the integral puts a cost to the control inputs and $\mathbf{R}$ are the control weights. The values of the three weighting matrices are selected depending on the desired performance of the system.

Solution to the regulator problem using Lagrange multipliers

There are several well-established solution processes for the general problem Equation (3.16). Here, we will present the solution using Lagrange multipliers of the regulator problem – which will serve also as a building block for LQR control in Section 5.3. Lagrange multipliers allow transforming the constrained optimization problem (3.16) into an unconstrained optimization problem. For that purpose, we defined the augmented cost

function

$$J_{aug}(\mathbf{x}(t), \mathbf{u}(t), \boldsymbol{\lambda}(t)) = J(\mathbf{x}(t), \mathbf{u}(t)) + \int_0^{t_f} \boldsymbol{\lambda}^\top \left[\mathbf{A}\mathbf{x} + \mathbf{B}\mathbf{u} - \dot{\mathbf{x}}\right] dt, \tag{3.21}$$

where $\boldsymbol{\lambda}(t)$ is the (unknown) vector of Lagrange multipliers, also known as *co-states*, which has the same size as the state vector. Note that, since the term between square brackets in Eq. (3.21) is zero for all time, the integrand is always zero for any bounded value of the Lagrange multipliers. As a result, minimizing the augmented cost function is equivalent to the minimization posed by (3.20). We will see that if the Lagrange multipliers are also considered as functions to be minimized against, the resulting problem also enforces the constraints given by the state equation (5.1).

Since the weight matrices are all positive, to obtain the minimum of J_{aug} we enforce that its variations are equal to zero, that is,

$$\begin{aligned} \delta J_{aug} = \mathbf{x}_f^\top \mathbf{H} \boldsymbol{\delta x}_f + \int_0^{t_f} \left[\mathbf{x}^\top \mathbf{Q} \boldsymbol{\delta x} + \mathbf{u}^\top \mathbf{R} \boldsymbol{\delta u}\right] dt \\ + \int_0^{t_f} \boldsymbol{\lambda}^\top \left[\mathbf{A}\boldsymbol{\delta x} + \mathbf{B}\boldsymbol{\delta u} - \boldsymbol{\delta \dot{x}}\right] dt + \int_0^{t_f} \boldsymbol{\delta \lambda}^\top \left[\mathbf{A}\mathbf{x} + \mathbf{B}\mathbf{u} - \dot{\mathbf{x}}\right] dt = 0. \end{aligned} \tag{3.22}$$

The time derivatives $\boldsymbol{\delta \dot{x}}$ are removed by using integration by parts. Noting that it must be $\boldsymbol{\delta x}(0) = \mathbf{0}$ and denoting $\boldsymbol{\lambda}(t_f) = \boldsymbol{\lambda}_f$, this results in

$$\begin{aligned} \delta J_{aug} = \boldsymbol{\delta x}_f^\top \left[\mathbf{H}\mathbf{x}_f - \boldsymbol{\lambda}_f\right] \\ + \int_0^{t_f} \boldsymbol{\delta x}^\top \left[\mathbf{Q}\mathbf{x} + \dot{\boldsymbol{\lambda}} + \mathbf{A}^\top \boldsymbol{\lambda}\right] dt \\ + \int_0^{t_f} \boldsymbol{\delta u}^\top \left[\mathbf{R}\mathbf{u} + \mathbf{B}^\top \boldsymbol{\lambda}\right] dt \\ + \int_0^{t_f} \boldsymbol{\delta \lambda}^\top \left[\mathbf{A}\mathbf{x} + \mathbf{B}\mathbf{u} - \dot{\mathbf{x}}\right] dt = 0. \end{aligned} \tag{3.23}$$

This equation has to be satisfied for any variations of the independent variables, i.e., $\boldsymbol{\delta x}$, $\boldsymbol{\delta u}$, $\boldsymbol{\delta \lambda}$, and the terminal conditions $\boldsymbol{\delta x}_f$. That results in four equations that will provide a solution to our optimization problem. Note that the last integral enforces the original state equations. From the second integral we obtain a relation for the input vector

$$\mathbf{u} = -\mathbf{R}^{-1}\mathbf{B}^\top \boldsymbol{\lambda}, \tag{3.24}$$

and the Lagrange multipliers are solved simultaneously with the state variable, by virtue of the first and third integral equations. After substituting the input vector using Eq. (3.24), we have

$$\begin{Bmatrix} \dot{\mathbf{x}} \\ \dot{\boldsymbol{\lambda}} \end{Bmatrix} = \begin{bmatrix} \mathbf{A} & -\mathbf{B}\mathbf{R}^{-1}\mathbf{B}^\top \\ -\mathbf{Q} & -\mathbf{A}^\top \end{bmatrix} \begin{Bmatrix} \mathbf{x} \\ \boldsymbol{\lambda} \end{Bmatrix}. \tag{3.25}$$

This system is sometimes referred to as the *Hamiltonian system*. It needs to be solved subject together with the initial conditions on the state variables, but the first right-hand-side term in Eq. (3.23) imposes terminal conditions on the Lagrange multiplier, that is,

$$\begin{aligned} \mathbf{x}(0) &= \mathbf{x}_0, \\ \boldsymbol{\lambda}(t_f) &= \mathbf{H}\mathbf{x}_f. \end{aligned} \tag{3.26}$$

As a result, solving for the state and co-state vectors implies marching forward and backwards in time, respectively. This problem is typically solved using *shooting methods*, in which a guess value of the co-states is assumed for $t = 0$, with a correcting mechanism to enforce the terminal condition at $t = t_f$. For small problems it can be solved by hand, as in the example below.

An analytical example

Consider the simple one-dimensional system

$$\dot{x}(t) = x(t) + u(t), \tag{3.27}$$

with initial conditions $x(0) = x_0$ and cost function with $H = 2$, $Q = 3$, and $R = 1$, that is,

$$J = x^2(T) + \frac{1}{2}\int_0^T \left(3x^2 + u^2\right) \mathrm{d}t, \tag{3.28}$$

and $T = 2$. We can derive the Hamiltonian system from the augmented cost function

$$J_{aug}(x(t), u(t), \lambda(t)) = x^2(T) + \frac{1}{2}\int_0^T \left(3x^2 + u^2\right) \mathrm{d}t + \int_0^T \lambda\left(x + u - \dot{x}\right) \mathrm{d}t \tag{3.29}$$

And the minimum of J_{aug} (the optimality condition) is then defined from enforcing $\delta J_{aug} = 0$ for any perturbations, that is,

$$\delta J_{aug} = 2x(T)\delta x(T) + \int_0^T \left[3x\delta x + u\delta u + \delta\lambda\left(x + u - \dot{x}\right) + \lambda\left(\delta x + \delta u - \delta\dot{x}\right)\right] \mathrm{d}t \tag{3.30}$$

After integration by parts in the final term in the equation, and using that $\delta x(0) = 0$,

$$\begin{aligned} \delta J_{aug} = {} & 2x(T)\delta x(T) - \lambda(T)\delta x(T) \\ & + \int_0^T \left[3x\delta x + u\delta u + \delta\lambda\left(x + u - \dot{x}\right) + \lambda\delta x + \lambda\delta u + \dot{\lambda}\delta x\right] \mathrm{d}t \end{aligned} \tag{3.31}$$

The corresponding Hamiltonian system is

$$\begin{Bmatrix} \dot{x} \\ \dot{\lambda} \end{Bmatrix} = \begin{bmatrix} 1 & -1 \\ -3 & -1 \end{bmatrix} \begin{Bmatrix} x \\ \lambda \end{Bmatrix} = \mathbf{A}_h \begin{Bmatrix} x \\ \lambda \end{Bmatrix}. \tag{3.32}$$

Solutions to this equation can be obtained via the matrix exponential

$$\begin{Bmatrix} x \\ \lambda \end{Bmatrix} = e^{\mathbf{A}_h t} \begin{Bmatrix} x_0 \\ \lambda_0 \end{Bmatrix}. \tag{3.33}$$

This is known as the *state transition matrix* and can be easily obtained here using symbolic algebra in Matlab[1] as

$$e^{\mathbf{A}_h t} = \frac{1}{4} \begin{bmatrix} e^{-2t} + 3e^{2t} & e^{-2t} - e^{2t} \\ 3e^{-2t} - 3e^{2t} & 3e^{-2t} + e^{2t} \end{bmatrix}. \tag{3.34}$$

Once the state-transition matrix is known, the terminal conditions, $\lambda(T) = Hx(T)$, can be used to define an equation in λ_0. Substituting $T = 2$ above gives

$$\begin{aligned} x(T) &= 40.95x_0 - 13.65\lambda_0, \\ \lambda(T) &= -40.93x_0 + 13.66\lambda_0, \end{aligned} \tag{3.35}$$

and, therefore

$$-40.93x_0 + 13.66\lambda_0 = 2\left(40.95x_0 - 13.65\lambda_0\right). \tag{3.36}$$

Solving gives $\lambda_0 = 1.0005x_0$, and therefore, for any given x_0 we can now integrate the Hamiltonian system (3.32) to obtain the optimal trajectory of x.

3.3 Further reading

Additional information on flight performance and steady manoeuvres can be found in the books by Stengel (2004) and Filippone (2012). For an introduction to manoeuvre loads, see Wright and Cooper (2007), and for their impact in vehicle design, see Niu (1999). An excellent introduction to optimal control for aerospace applications can be found in the classic book of Kirk (1970).

[1] This approach is only feasible for small problems and it is known as the *direct solution*. For larger systems, numerical integration is required.

Chapter 4

Flexible-Aircraft Equations of Motion

We will consider next the dynamics of aircraft that deform under the aerodynamic forces, and the impact that this has in the vehicle flight peformance. It will be assumed that the typical time scales in the aircraft vibrations (defined by its lowest natural frequency) are much higher than those in the flight dynamics, which is the usual case in most aircraft. The description of the flexible aircraft dynamics with quasi-static structural response builds directly on the rigid-aircraft dynamic description of Chapter 1, and the general structure of the resulting *elastified* aircraft flight dynamics is described here, alongside some examples.

4.1 Aircraft dynamics with quasi-static deformations

irst, additional degrees of freedom that describe the instantaneous deformed state, and, second, additional equations that determine their values. In general, this is an infinite-dimensional problem described by partial-differential equations, however, for all practical purpose it is approximated by a finite-dimensional representation. Consequently, the instantaneous deformed state of the aircraft will be described by a vector $\mathbf{x}_s(t)$ of structural degrees of freedom that is defined from a discrete representation of the airframe structure (typically, a finite-element model). Its definition will be made specific in subsequent sections, and the only condition here is that $\mathbf{x}_s(t)$ describes the deformed airframe geometry with respect a certain reference point, which will be chosen as the origin of the reference frame used to describe its rigid-body dynamics. For consistency with the description in Chapter 1, this will be chosen as the the aircraft center of mass, although this is not strictly necessary – although it is common practice regardless. In such case, Equation (1.26) needs to be modified to include the effect of the instantaneous aircraft

geometry, as

$$\dot{\mathbf{x}}_r = \mathfrak{f}_{gyr}^{(r)}(\mathbf{x}_r) + \mathfrak{f}_{grav}^{(r)}(\mathbf{x}_r) + \mathfrak{f}_{aero}^{(r)}(\mathbf{x}_r, \mathbf{x}_s, \mathbf{u}) + \mathfrak{f}_{prop}^{(r)}(\mathbf{x}_r, \mathbf{x}_s, \mathbf{u}), \tag{4.1}$$

where we have added the superscript $\bullet^{(r)}$ to the forcing terms to indicate that they correspond to the force and moment resultants at the center of mass. A dependency of the resultant propulsive forces with the elastic degree of freedom has also been included to consider the case of wing-mounted engines, where wing deformations may change the orientation of the thrust vector. While a small wing twist, of the order of degrees, generates rather large changes on the aerodynamic forces, it does not effectively modify the mass distribution on the aircraft – and therefore the resultant gravitational forces. This situation is characteristic of most flexible air vehicles and, consequently, we assume here that the shape changes are not big enough to affect the evaluation of the resultant forces due to gravity. This also implies that the location of the center of gravity remains effectively unaltered by the aircraft deformations.

Note that, in general, the dimensions of $\mathbf{x}_s$, N_s, are much bigger than those of $\mathbf{x}_r$, $N_r << N_s$ (we need $N_r = 8$ degrees of freedom to describe the full rigid-aircraft flight dynamics, but we may have thousands of nodes in a finite-element model). To determine $\mathbf{x}_s$, we need information of the spatial distribution of the various external forces applied on the aircraft, e.g., it is not sufficient to know the value of the total lift to estimate the bending of the wings, which need instead information about the spanwise lift distribution. Under the small amplitude assumption, the structural deformations under those distributed forces are determined by the stiffness matrix of the structure, $\mathbf{K}_{ss}$, which is assumed to be known. In that case, the static equilibrium on the structure can be obtained in general as

$$\mathbf{K}_{ss}\mathbf{x}_s = \mathfrak{f}_{gyr}^{(s)}(\mathbf{x}_r) + \mathfrak{f}_{grav}^{(s)}(\mathbf{x}_r) + \mathfrak{f}_{aero}^{(s)}(\mathbf{x}_r, \mathbf{x}_s, \mathbf{u}) + \mathfrak{f}_{prop}^{(s)}(\mathbf{x}_r, \mathbf{x}_s, \mathbf{u}). \tag{4.2}$$

The terms of the right hand side are the discrete (nodal) forces generated by gyroscopic, gravity, aerodynamic and propulsion forces on the structure. In general, all those effects may contribute to deform the vehicle, but, in many cases, only the aerodynamic forces are usually relevant (and the propulsion forces for wing-mounted engines). Both Eqs. (4.1) and (4.2) depend on $\mathbf{x}_r$ and $\mathbf{x}_s$ and therefore they need to be solved simultaneously. The corresponding block diagram is shown in Figure 4.1.

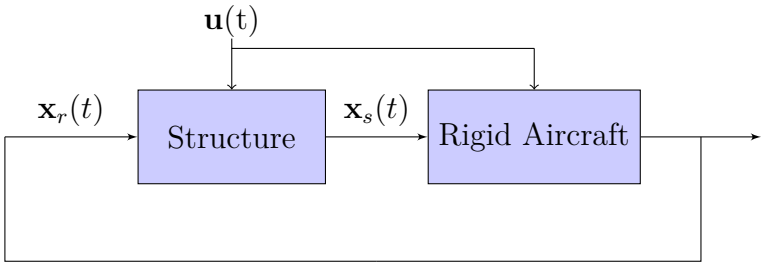

Figure 4.1: Interaction between rigid and flexible degrees of freedom.

For linear problems with reference around zero, Eqs. (4.1) and (4.2) become

$$\begin{aligned} \dot{\mathbf{x}}_r &= \mathbf{A}_{rr}\mathbf{x}_r + \mathbf{A}_{rs}\mathbf{x}_s + \mathbf{B}_r\mathbf{u}, \\ \mathbf{K}_{ss}\mathbf{x}_s &= \mathbf{A}_{sr}\mathbf{x}_r + \mathbf{A}_{ss}\mathbf{x}_s + \mathbf{B}_s\mathbf{u}. \end{aligned} \tag{4.3}$$

This is a differential-algebraic equations that simultaneously solves the structural and rigid-body degrees of freedom. Since the equations are linear, we can easily find a solution by first solving for $\Delta\mathbf{x}_s$ in the structural equation and then substituting back into the first one. This is equivalent to seeing the structural effects in Figure 4.1 as a constant feedback (a static gain) on the rigid-aircraft equations in a process known as *residualization* of the coupled equations. That gives

$$\dot{\mathbf{x}}_r = \bar{\mathbf{A}}_r\mathbf{x}_r + \bar{\mathbf{B}}_r\mathbf{u}, \tag{4.4}$$

with

$$\begin{aligned} \bar{\mathbf{A}}_r &= \mathbf{A}_{rr} + \mathbf{A}_{rs}\left(\mathbf{K}_{ss} - \mathbf{A}_{ss}\right)^{-1}\mathbf{A}_{sr}, \\ \bar{\mathbf{B}}_r &= \mathbf{B}_r + \mathbf{A}_{rs}\left(\mathbf{K}_{ss} - \mathbf{A}_{ss}\right)^{-1}\mathbf{B}_s. \end{aligned} \tag{4.5}$$

Matrices $\bar{\mathbf{A}}_r$ and $\bar{\mathbf{B}}_r$ are referred to as the "elastified" system and input matrices and describe the dynamics of a flexible aircraft. Therefore, using this elastified description we retain the original number of degrees of freedom of the rigid-aircraft problem, but with modified coefficients. Note that one actually only needs Eq. (4.2) to be linear to be able to eliminate the structural degrees of freedom in (4.1). This situation typically occurs under the small-displacement assumption and for attached-flow conditions. Finally, we can add an output equation to Eqs. (4.4), which would be similarly written as

$$\mathbf{y} = \bar{\mathbf{C}}_r\mathbf{x}_r + \bar{\mathbf{D}}_r\mathbf{u}. \tag{4.6}$$

What is included in $\mathbf{y}$ depends on the specific problem, but since our description "internally" solves for the structural degrees of freedom using the second of (4.3), the

output vector $\mathbf{y}$ can include structural (e.g. wing deformation measurements) as well as rigid-body information.

4.1.1 Divergence and control reversal

For $\bar{\mathbf{A}}_r$ and $\bar{\mathbf{B}}_r$ to exist, the inverse of $(\mathbf{K}_{ss} - \mathbf{A}_{ss})$ has to exist. Since, by definition, the structural degrees of freedom do not include rigid-body motions, $\mathbf{K}_{ss}$ is full rank. Matrix $\mathbf{A}_{ss}$ includes aerodynamic terms, and therefore its value will vary with the flight conditions. Whenever it is $\det(\mathbf{K}_{ss} - \mathbf{A}_{ss}) = 0$, one has aircraft *divergence*. A divergence velocity corresponds to points of structural failure and all points in the flight envelope need to be be at least 15% of any possible divergence condition.

There could also be flight conditions in which the control inputs in (4.4) have no authority on some of the aircraft degrees of freedom (this typically occur when one of the terms in $\bar{\mathbf{B}}_r$ becomes zero). Those are refered to as *uncontrollable states*. The flight condition at which this happens defines a point of *control reversal*.

4.2 Longitudinal dynamics of an aircraft with a flexible fuselage

As a first example, consider the longitudinal dynamics of an aircraft in steady climb with rigid wing and tail but with a flexible fuselage. The linear dynamics of this problem can be described in first approximation as in Chapter 2, with the effect of the flexible fuselage modelled by a rotational spring at a distance l_β from the tail, as shown in Figure 4.2. This results in an additional degree of freedom that will be chosen as the rotation angle, β, of the tail section with respect to main fuselage. This angle is assumed to be sufficiently small for a linear solution to this problem to be still valid.

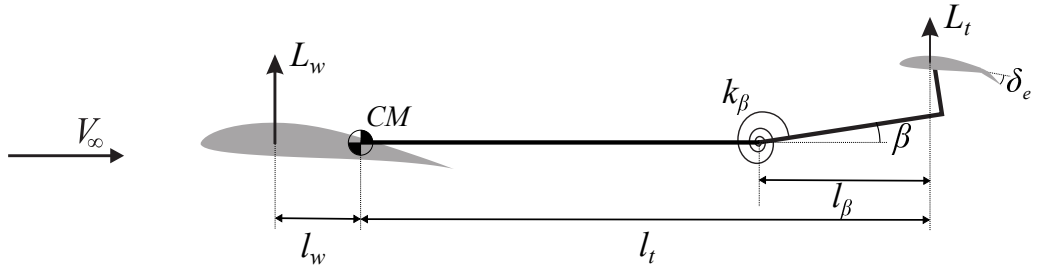

Figure 4.2: Geometry of an aircraft with a flexible hinge in the fuselage

If the natural frequency of the fuselage vibrations is much higher than the typical

frequencies in the rigid-body dynamics, Equation (2.3) are still valid for this problem. The instantaneous lift on the tail will however also be affected by the tail rotation, and becomes

$$\begin{aligned}
\Delta C_L &= C_{L\alpha}\frac{v_z}{V_\infty} + \frac{S_t}{S}C^t_{L\alpha}\left(\frac{l_t\omega_y}{V_\infty} - \beta\right) + \frac{S_t}{S}C^t_{L\delta}\delta_e, \\
\Delta C_D &= \frac{2SC_{L0}C_{L\alpha}}{\pi b^2 e}\frac{v_z}{V_\infty}, \\
\Delta C_{M_y} &= \left(\frac{l_w}{c}C^w_{L\alpha} - \frac{S_t l_t}{Sc}C^t_{L\alpha}\right)\frac{v_z}{V_\infty} - \frac{S_t l_t}{Sc}C^t_{L\alpha}\left(\frac{l_t\omega_y}{V_\infty} - \beta\right) - \frac{S_t l_t}{Sc}C^t_{L\delta}\delta_e,
\end{aligned} \tag{4.7}$$

where, as before, v_z and ω_y are the normal and angular velocities of the center of mass, CM. If we further assume that it is $\beta = 0$ at the equilibrium condition (the aircraft trimmed for steady climb), then the fuselage rotation in the subsequent aircraft dynamics is determined by the instantaneous equilibrium of moments at the hinge, that is,

$$k_\beta\beta = l_\beta L_t = \frac{1}{2}\rho_\infty V_\infty^2 S_t l_\beta\left[C^t_{L\alpha}\left(\frac{v_z}{V_\infty} + \frac{l_t\omega_y}{V_\infty} - \beta\right) + C^t_{L\delta}\delta_e\right]. \tag{4.8}$$

This results in the following equations of motions for the flexible aircraft,

$$\begin{aligned}
\dot{\mathbf{x}}_r &= \mathbf{A}_r\mathbf{x}_r + \mathbf{A}_{rs}\beta + \mathbf{B}_r\delta_e, \\
k_\beta\beta &= A_s\beta + \mathbf{A}_{sr}\mathbf{x}_r + B_s\delta_e,
\end{aligned} \tag{4.9}$$

with $\mathbf{x}_r = \left(v_x, v_z, \omega_, \theta\right)^\top$, $\mathbf{A}_r$ and $\mathbf{B}_r$ still given by Equations (2.17) and (2.18), respectively, and with the new coefficients

$$\begin{aligned}
A_s &= -\frac{1}{2}\rho_\infty V_\infty^2 S_t l_\beta C^t_{L\alpha}, \\
\mathbf{A}_{rs} &= \frac{\rho_\infty V_\infty^2 S_t C^t_{L\alpha}}{2m}\begin{bmatrix}0 & 1 & \frac{l_t m}{I_{yy}} & 0\end{bmatrix}^\top, \\
\mathbf{A}_{sr} &= \frac{1}{2}\rho_\infty V_\infty S_t l_\beta C^t_{L\alpha}\begin{bmatrix}0 & 1 & l_t & 0\end{bmatrix}, \\
B_s &= \frac{1}{2}\rho_\infty V_\infty S_t l_\beta C^t_{L\delta}.
\end{aligned} \tag{4.10}$$

As in the general case, under quasi-steady approximations, the "elastification" of the solution consists on augmenting the rigid-body equations with dependencies to the elastic degree of freedom. We can solve for β as a function of the rigid-body states and inputs using the second equation in Equation (4.9), which gives a solution of the form of

Equation (4.4), that is,

$$\dot{\mathbf{x}}_r = \left(\mathbf{A}_r + \frac{1}{k_\beta - A_s}\mathbf{A}_{rs}\mathbf{A}_{sr}\right)\mathbf{x}_r + \left(\mathbf{B}_r + \frac{B_s}{k_\beta - A_s}\mathbf{A}_{rs}\right)\delta_e. \tag{4.11}$$

As it is $k_\beta - A_s = k_\beta + \frac{1}{2}\rho_\infty V_\infty^2 S_t l_\beta C_{L\alpha}^t > 0$, there is no divergence at any airspeed. Note however that if l_β was negative (e.g., the tail was in canard configuration), then aeroelastic divergence could be found if the fuselage was sufficiently flexible.

4.3 Roll control of flexible straight wings

Roll response is a typical situation in which wing flexibility affects aircraft dynamics. In this final section we will construct a simple model to exemplify the key characteristics in this problem. The vehicle's linearized dynamics, starting from level flight reference conditions, will be determined by the lateral equations in (2.3) with $\Theta_0 = 0$, which become

$$\begin{aligned} m\dot{v}_y &= F_y + mg\phi - mV_\infty\omega_z, \\ I_{xx}\dot{\omega}_x - I_{xz}\dot{\omega}_z &= M_x, \\ -I_{xz}\dot{\omega}_x + I_{zz}\dot{\omega}_z &= M_z, \\ \dot{\phi} &= \omega_x. \end{aligned} \tag{4.12}$$

The terms in this equation can be matched to the general formulation in eq. (4.1). The rigid-body state vector is $\mathbf{x}_r = \left(v_x, \omega_x, \omega_y, \phi\right)^\top$. Linearized gravity and gyroscopic forces only appear in the first equation in (4.12). Finally, Fy, M_x and M_z, will in general represent the aerodynamic and propulsion lateral force and roll and yaw moments, respectively, which will be know a function of the aircraft rigid-body velocities, control and thrust inputs, but also of the structural deformations.

In the rest of this chapter a simplified model will be considered: the vehicle will be assumed to have large high-aspect-ratio straight wings of semi-span b, such that the fuselage dimensions become negligible, and full-span ailerons, as shown in fig. 4.3. The effect of thrust forces in the lateral dynamics will be also considered neglibible. For a positive roll (when there is no control reversal), the aileron deflection will be negative on the right wing and positive on the left wing, that is,

$$\begin{aligned} \delta_a &= -\delta_a^* \quad \text{for} \quad y > 0, \\ \delta_a &= \delta_a^* \quad\;\; \text{for} \quad y < 0. \end{aligned} \tag{4.13}$$

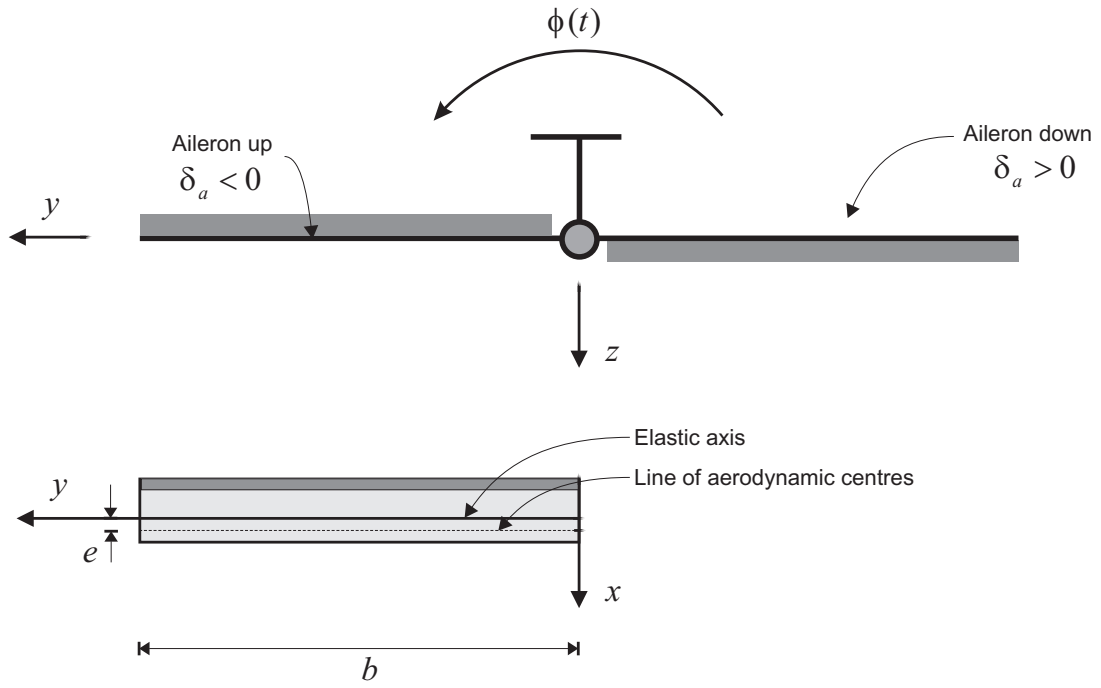

Figure 4.3: Simplified model for roll control of a flexible aircraft (front view of the full aircraft and plant view of the wing).

To evaluate the aerodynamic forces and moments in eq. (4.12), we will first need model for the structural response of the wings as well as for the distribution of aerodynamic loads on the wings (which are the cause of their deformations). Next, from the aeroelastic equilibrium between them we will be able to obtain the resultant aerodynamic forces that drive the aircraft dynamics. This is done next.

4.3.1 Structural Model: Torque tube

The flexibility of the wing can be modelled in first approximation as a beam with torsional stiffness $GJ(y)$[1]. We will further assume that the elastic axis, around which the sections rotate in torsion without vertical displacement,coincides with the spanwise vehicle stability axis, y, as show in fig. 4.3.

As discussed above, we will consider quasi-static structural response. If the wing is subject to a twisting moment per unit length $\tau(y)$, which will be due to the aerodynamic lift/moment distribution along the wing (and, in general, also to the propulsion forces with wing-mounted engines) then the torsional equilibrium of the wing is determined by

[1]Wings are normally stiffer at the root than at the tip and the stiffness constant will vary along the wing span

the solution of the differential equation

$$\frac{d}{dy}\left(GJ(y)\frac{d\theta}{dy}\right)+\tau(y)=0, \tag{4.14}$$

where $\theta(y)$ is the elastic twist angle. It is defined such that a positive elastic twist pitches up the starboard (right) wing. Equation (4.14) needs to be solved together with the boundary conditions of the problem, which, for a cantilever wing, are

$$\begin{aligned}\theta(0)&=0,\\ \theta'(b)&=0.\end{aligned} \tag{4.15}$$

Equation (4.14) can also be written in weak form, as

$$\int_0^b \left(\delta\theta' GJ\theta' - \delta\theta\tau\right) dy = 0, \tag{4.16}$$

with $\delta\theta$ and arbitrary virtual rotation field that satisfies the natural boundary conditions (that is, $\delta\theta(0)=0$ for a cantilever beam). This form of the equation is very suitable for numerical approximations. For the examples here we will approximate the rotation and virtual rotation distributions by a set of known *test functions*, defined by a row vector $\mathbf{N}(y)$ of dimension N_s, such that

$$\begin{aligned}\theta(y)&\approx\mathbf{N}(y)\mathbf{x}_s,\\ \delta\theta(y)&\approx\mathbf{N}(y)\delta\mathbf{x}_s.\end{aligned} \tag{4.17}$$

Examples of test functions are Fourier series, in which case $\mathbf{x}_s$ is the amplitude of the modes, or piecewise linear interpolating functions in a finite-element discretization, in which case $\mathbf{x}_s$ is the nodal rotations. Substituting into Equation (4.16) and canceling $\delta\mathbf{x}_s$ that multiplies both terms of the equations, gives

$$\mathbf{K}_{ss}\mathbf{x}_s=\mathfrak{f}_{aero}^{(s)}, \tag{4.18}$$

with

$$\begin{aligned}\mathbf{K}_{ss}&=\int_0^b \mathbf{N}'^{\top}(y)GJ(y)\mathbf{N}'(y)\mathrm{d}y,\\ \mathfrak{f}_{aero}^{(s)}&=\int_0^b \mathbf{N}^{\top}(y)\tau(y)\mathrm{d}y.\end{aligned} \tag{4.19}$$

This is the approximation to eq. (4.2) for the case of a single structural degree of freedom.

4.3.2 Aerodynamic model: Thin-strip theory

We will ignore the effect of the constant angle of attack of the wing, since it is a symmetric effect and only antisymmetric aerodynamic forces will generate roll. The aerodynamic force and moment coefficients (about the aerodynamic centre) on each wing section due to δ_a (positive down) are determined by the aerofoil geometry. For trailing-edge control surfaces, it is $c_{l\delta} > 0$ and $c_{m\delta} < 0$. The lift-curve slope of the aerofoils, $c_{l\alpha}$ is also known. In general, the elastic axis, which depends on the internal layout of the wing, and the aerodynamic centre, which depends of the external geometry, will not coincide. This is shown in Figure 4.3 where the distance between both axis is defined by the parameter e, which will be positive when the aerodynamic centre is ahead of the elastic axis. If the aircraft has a rolling rate of $\dot{\phi}$ due to the ailerons then at any station y the vertical velocity due to roll will be $y\dot{\phi}$ (positive downwards along the right wing). This effectively changes the angle of incidence, as shown in Figure 4.4.

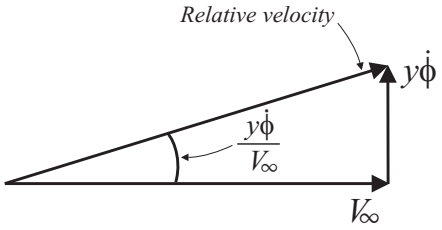

Figure 4.4: Increase in incidence angle for the right wing with positive roll rate.

If the local chord is $c(y)$, and under the strip-theory assumption, we have the following lift and moment about the aerofoil's aerodynamic centre (both per unit length) at a location y along the wing span,

$$\begin{aligned} l(y) &= q_\infty c \left[c_{l\alpha} \left(\theta + \frac{y\dot{\phi}}{V_\infty} \right) - c_{l\delta} \delta_a^* \right], \\ m_{ac}(y) &= -q_\infty c^2 c_{m\delta} \delta_a^*. \end{aligned} \tag{4.20}$$

These equations are for the right wing ($y > 0$). At the left wing ($y < 0$) the distributions of lift and aerodynamic moment will be equal but with opposite sign. The different contributions to the wing lift distribution are shown in Figure 4.5. Note that a positive value of $\theta(y)$ implies that the elastic deformation of the wing reduces the effectiveness of the aileron.

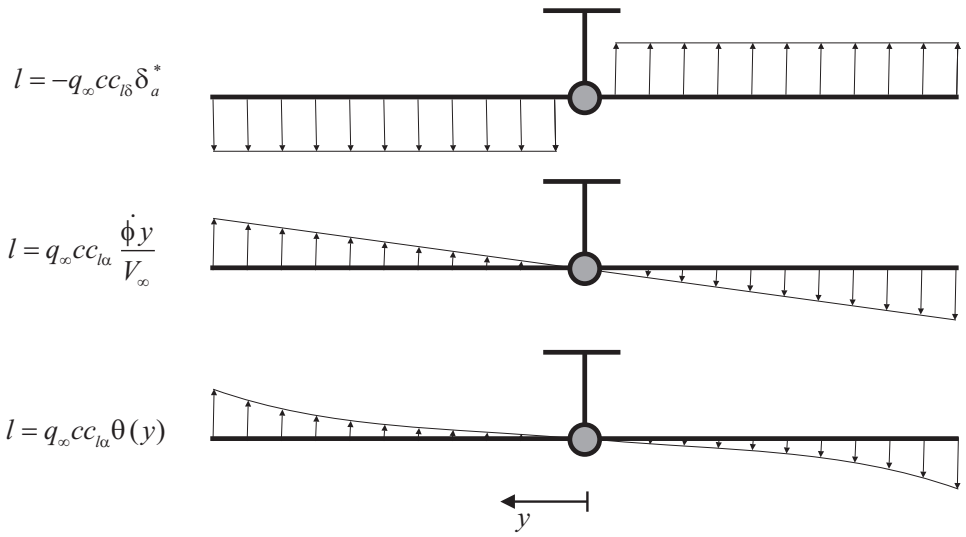

Figure 4.5: Contributions to wing lift distribution in flexible aircraft in roll.

Finally, the torsional moment generated on the right wing by the incremental aerodynamic forces in the rolling manoeuvre is

$$\tau(y) = el + m_{ac}. \tag{4.21}$$

with the lift and moment per unit length given by Eq. (4.20).

4.3.3 Aeroelastic equilibrium

Once the torsional moment $\tau(y)$ generated by the aerodynamic forces is obtained, we can solve the structural equations. These integrals depend on known parameters and can be numerically evaluated for a given problem. Solving now for $\mathbf{x}_s$, we have

$$\begin{aligned} \mathbf{K}_{ss}\mathbf{x}_s &= \int_0^b \mathbf{N}^\top \left(el(y) + m_{ac}(y)\right) \mathrm{d}y \\ &= q_\infty \int_0^b \mathbf{N}^\top \left[ec_{l\alpha} \left(\theta + \frac{y\dot{\phi}}{V_\infty} \right) - \left(ec_{l\delta} + cc_{m\delta} \right) \delta_a^* \right] c \mathrm{d}y. \end{aligned} \tag{4.22}$$

Substituting $\theta(y) = \mathbf{N}(y)\mathbf{x}_s$ and integrating

$$\mathbf{K}_{ss}\mathbf{x}_s = q_\infty \left(\boldsymbol{\mathcal{A}}_{ss}\mathbf{x}_s + \boldsymbol{\mathcal{A}}_{sr} \frac{b\dot{\phi}}{V_\infty} + \boldsymbol{\mathcal{A}}_{su}\delta_a^* \right) \tag{4.23}$$

with the matrices in the problem defined as

$$\begin{aligned}\boldsymbol{\mathcal{A}}_{ss} &= \int_0^b \mathbf{N}^\top ecc_{l\alpha}\mathbf{N}\,\mathrm{d}y,\\ \boldsymbol{\mathcal{A}}_{sr} &= \int_0^b \mathbf{N}^\top \frac{yec}{b}c_{l\alpha}\,\mathrm{d}y,\\ \boldsymbol{\mathcal{A}}_{su} &= -\int_0^b \mathbf{N}^\top (ecc_{l\delta} + c^2 c_{m\delta})\,\mathrm{d}y.\end{aligned} \tag{4.24}$$

We can now solve the elastic variables, $\mathbf{x}_s$, in terms of the rigid-body variables, δ_a^* and $\dot{\phi}$, as

$$\theta(y) = q_\infty \mathbf{N}(y)\left(\mathbf{K}_{ss} - q_\infty \boldsymbol{\mathcal{A}}_{ss}\right)^{-1}\left(\boldsymbol{\mathcal{A}}_{sr}\frac{b\dot{\phi}}{V_\infty} + \boldsymbol{\mathcal{A}}_{su}\delta_a^*\right). \tag{4.25}$$

Note that for this equation to have a solution, it must be $\det(\mathbf{K}_{ss} - q_\infty \boldsymbol{\mathcal{A}}_{ss}) \neq 0$, that is, the dynamic pressure must be below the vehicle's reversal dynamic pressure (if a positive value of q_D does exist). Finally, the total rolling moment, M_x generated on the aircraft from both wings can be now obtained by integration of the lift in Equation (4.20). Using the symmetry of the problem, we need to integrate only along one wing, which results in

$$\begin{aligned}M_x &= -2\int_0^b yl(y)\,\mathrm{d}y = \\ &= 2q_\infty \int_0^b ycc_{l\delta}\delta_a^*\,\mathrm{d}y - 2q_\infty \int_0^b ycc_{l\alpha}\left(\mathbf{N}\mathbf{x}_s + \frac{y\dot{\phi}}{V_\infty}\right)\mathrm{d}y\end{aligned} \tag{4.26}$$

where, after introducing a reference chord c_0, we can explicitly carry out both integrals for a given configuration, as

$$M_x = q_\infty c_0 b^2\left[C_\delta \delta_a^* + C_{\dot{\phi}}\frac{b\dot{\phi}}{V_\infty}\right], \tag{4.27}$$

Two dimensionless *elastified* aerodynamic derivatives, $C_{\dot{\phi}}$, and C_δ, have been defined in this expression, as

$$\begin{aligned}C_\delta &= \frac{2}{b^2 c_0}\int_0^b ycc_{l\delta}\,\mathrm{d}y - \frac{2q_\infty}{b^2 c_0}\int_0^b ycc_{l\alpha}\mathbf{N}\left(\mathbf{K}_{ss} - q_\infty\boldsymbol{\mathcal{A}}_{ss}\right)^{-1}\boldsymbol{\mathcal{A}}_{su}\,\mathrm{d}y,\\ C_{\dot{\phi}} &= -\frac{2}{b^3 c_0}\int_0^b y^2 cc_{l\alpha}\,\mathrm{d}y - \frac{2q_\infty}{b^2 c_0}\int_0^b ycc_{l\alpha}\mathbf{N}\left(\mathbf{K}_{ss} - q_\infty\boldsymbol{\mathcal{A}}_{ss}\right)^{-1}\boldsymbol{\mathcal{A}}_{sr}\,\mathrm{d}y.\end{aligned} \tag{4.28}$$

The first integral in both definitions corresponds to the rigid-aircraft aerodynamics, which depends solely on the aerodynamic properties of the wing airfoils and the wing geometry. The rigid-body contributions are positive in C_δ and negative in $C_{\dot{\phi}}$ (in particular,

due to the normalization in Equation (4.27), they are also independent of the dynamic pressure). The second integral includes the aeroelastic effects, which depend additionally on the structural characteristics of the wing and, importantly, on the dynamic pressure. In aircraft wings, the elastic axis is typically behind the aerodynamic axis ($e > 0$ in Figure 4.3). In such a case, positive lift on a wing section generates a pitch up moment, and therefore positive values of the torsional angle. As a result the usual situation is for the elastic contribution in both C_δ and $C_{\dot{\phi}}$ to be negative, and increasingly so with the dynamic pressure.

Therefore, the usual situation is for C_δ to be positive at low dynamic pressures and negative for sufficiently high speeds. There is a dynamic pressure for which $C_\delta = 0$, for which aileron deflections do not generate rolling moments (a *control reversal* condition). This will be exemplified below on a wing with constant properties, for which analytical solutions of this problem can be obtained.

4.3.4 Elastic effects in the roll response

In the previous section we have obtained a model for the rolling moment of a flexible wing. At airspeeds below the control reversal limit, this can then be fed into the EoM of the aircraft to determine the transient dynamics of the vehicle. For simplicity, we will assume that the inertia tensor is diagonal, in which case the lateral response of the aircraft is determined by

$$\begin{aligned} I_{xx}\dot{\omega}_x &= M_x, \\ \dot{\phi} &= \omega_x. \end{aligned} \tag{4.29}$$

With the expression of the roll moment obtained above, this results in

$$\begin{Bmatrix} \dot{\omega}_x \\ \dot{\phi} \end{Bmatrix} = \begin{bmatrix} \frac{q_\infty c b^3 C_{\dot{\phi}}}{V_\infty I_{xx}} & 0 \\ 1 & 0 \end{bmatrix} \begin{Bmatrix} \omega_x \\ \phi \end{Bmatrix} + \begin{Bmatrix} \frac{q_\infty c b^2 C_\delta}{I_{xx}} \\ 0 \end{Bmatrix} \delta_a^*. \tag{4.30}$$

This equation corresponds to eq. (4.4) for this simplified problem. As before, e can represent the effect of flexibility in the response to the aileron inputs by means of the block diagram with the flexibility as a constant gain feedback, which now looks as in Figure 4.6.

In this particular case, the problem can be directly written in terms of the roll angle and its derivatives, as

$$I_{xx}\ddot{\phi} - q_\infty \frac{c b^3 C_{\dot{\phi}}}{V_\infty}\dot{\phi} = q_\infty c b^2 C_\delta \delta_a \tag{4.31}$$

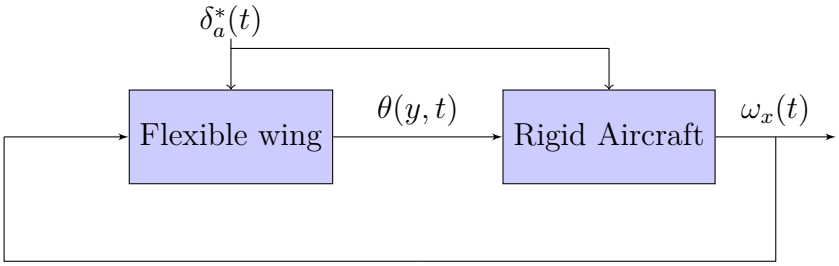

Figure 4.6: Block diagram for roll control with flexible wings.

Note that, since $C_{\dot{\phi}} < 0$, the damping term is always positive. This equation can now be solved for any input on the aileron, which will be defined by either pilot or FCS commands. Of particular importance is the steady-state roll rate, which is obtained by imposing $\ddot{\phi} = 0$. In that case it is $\dot{\phi}^* = -\frac{V_\infty C_\delta}{bC_{\dot{\phi}}}\delta_a^*$. The effect of the aileron depends on C_δ, which enhances roll authority, and $C_{\dot{\phi}}$, which decreases it. However, changes in C_δ with dynamic pressure are typically much higher than in $C_{\dot{\phi}}$ and thus the torsional flexibility of the wing has an overall detriment effect on the roll authority as the aircraft flies faster.

Chapter 5

Optimal feedback control

The Flight Control System (FCS) is an essential component in any modern aircraft. It consists of a set of physical sensors and actuators, distributed throughout the vehicle, as well as the control logic, which is implemented in on-board computer systems (although, particularly for UAVs, often ground-based computers are an integral part of the FCS). Sensors, such as Pitot tube measurements or the Inertial Measurement Unit (IMU), are used to *estimate* the current state of the system. In this course we will assume that they provide perfect knowledge of the instantaneous system state (full state feedback), although in practice state estimation is a key ingredient in control system design. The actuators are the control surfaces and throttle setting defined in section 1.3.

Figure 5.1: Block diagram for open-loop aircraft dynamics with disturbance inputs.

FCS can be designed to improve the handling qualities of the aircraft, by, for instance, providing *stability augmentation*. This is mainly achieved by placing the closed-loop system eigenvalues at more "pilot-friendly" locations in the complex plane, compared to where they would be for the aircraft operating in open-loop.

FCS can also be designed to keep the aircraft in a certain trajectory, by compensating against disturbances (e.g., atmospheric turbulence). In this case, the control system acts as a *regulator*. The linear system dynamics in this case is written as eq. (2.3) and is represented in Figure 5.1. The disturbance may be due to atmospheric turbulence, but also to errors in the actuator inputs (e.g., the actual aileron deflection is not exactly the commanded one). There may be no *a priori* information about the values of $\mathbf{w}(t)$, but often we know some general characteristics of it that can be used to improve the

effectiveness of the controller.

5.1 The Linear Quadratic Regulator

The focus here will be on controller design using *optimal control theory*, which was already introduced to define optimal trajectories in Section 3.2.2. While classical analytical methods are better suited for single-input single-output (SISO) systems, the definition of the control design as the solution of an optimization problem expanded the application to more general multi-input multi-output (MIMO) problems.

The Linear Quadratic Regulator (LQR) obtains the control signal by means of an optimization problem on the state-equations with full-state feedback, non-zero initial conditions, no disturbance inputs and a quadratic performance index[1]. Without loss of generality, we will also assume that the reference state is zero. This situation is schematically shown in Figure 5.2. The linearised vehicle dynamics is then given by state equations such as Eq. (2.16). For full-state feedback, they become

$$\begin{aligned} \dot{\mathbf{x}} &= \mathbf{A}\mathbf{x} + \mathbf{B}\mathbf{u}, \\ \mathbf{y} &= \mathbf{x}. \end{aligned} \tag{5.1}$$

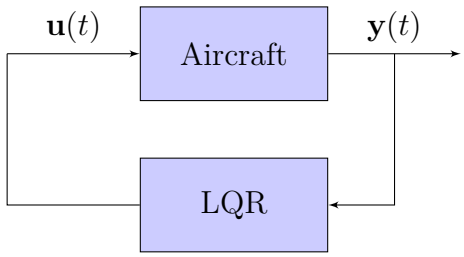

Figure 5.2: Block diagram for closed-loop aircraft dynamics with LQR control.

An LQR controller minimizes a quadratic *cost function* (also known as performance index) of the inputs and system states over a given time horizon, t_f, of the form of Equation (3.20), with the difference that now it will establish a feedback between the current states and the input. It does this by postulating the existence of a symmetric matrix function $\mathbf{P}(t)$ that at all times satisfies $\boldsymbol{\lambda}(t) = \mathbf{P}(t)\mathbf{x}(t)$. Since $\boldsymbol{\lambda}(t)$ is algebraically related to the input vector $\mathbf{u}(t)$ from Eq. (3.24), this assumption implies that the optimal

[1]This is an important distinction: controller design is done on certain test conditions or on a simplified model of the physical system, but it is expected to operate on the real physical system itself. In the design of the LQR we assume a perfect system with no disturbances.

control input can be obtained from the state vector as

$$\mathbf{u}(t) = -\mathbf{R}^{-1}\mathbf{B}^\top \mathbf{P}(t)\mathbf{x}(t). \tag{5.2}$$

An equation for $\mathbf{P}(t)$ is obtained by taking differentiating $\boldsymbol{\lambda}(t) = \mathbf{P}(t)\mathbf{x}(t)$ with time, as

$$\dot{\boldsymbol{\lambda}} = \dot{\mathbf{P}}\mathbf{x} + \mathbf{P}\dot{\mathbf{x}}. \tag{5.3}$$

Substituting $\dot{\mathbf{x}}$ and $\dot{\boldsymbol{\lambda}}$ from Eq. (3.25), we then have

$$\dot{\mathbf{P}}\mathbf{x} + \mathbf{P}\left(\mathbf{A}\mathbf{x} - \mathbf{B}\mathbf{R}^{-1}\mathbf{B}^\top\boldsymbol{\lambda}\right) - \left(-\mathbf{Q}\mathbf{x} - \mathbf{A}^\top\boldsymbol{\lambda}\right) = 0. \tag{5.4}$$

If we finally replace $\boldsymbol{\lambda} = \mathbf{P}\mathbf{x}$, we have

$$\left(\dot{\mathbf{P}} + \mathbf{P}\mathbf{A} + \mathbf{A}^\top\mathbf{P} + \mathbf{Q} - \mathbf{P}\mathbf{B}\mathbf{R}^{-1}\mathbf{B}^\top\mathbf{P}\right)\mathbf{x} = 0. \tag{5.5}$$

This equation holds for any initial condition $\mathbf{x}(0) = \mathbf{x}_0$. Since by varying the initial condition we can obtain any value of $\mathbf{x}(t)$, then it has to be

$$\dot{\mathbf{P}} + \mathbf{P}\mathbf{A} + \mathbf{A}^\top\mathbf{P} + \mathbf{Q} - \mathbf{P}\mathbf{B}\mathbf{R}^{-1}\mathbf{B}^\top\mathbf{P} = 0. \tag{5.6}$$

This is matrix equation (which as many independent equations as coefficients in the symmetric matrix $\mathbf{P}$), which known as the *Riccati equation*. Since $\boldsymbol{\lambda}$ and $\mathbf{x}$ have to satisfy the terminal condition at $t = t_f$ given in Eq. (3.26), the Riccati equation actually needs to be integrated backwards in time from the condition $\mathbf{P}(t_f) = \mathbf{H}$. Substituting in Eq. (3.24) finally provides the optimal control input (the *optimal gains*) as

$$\mathbf{u}(t) = -\mathbf{R}^{-1}\mathbf{B}^\top \mathbf{P}(t)\mathbf{x}(t). \tag{5.7}$$

This defines the time-varying feedback gain matrix $\mathbf{K}(t) = -\mathbf{R}^{-1}\mathbf{B}^\top\mathbf{P}(t)$ that closes the loop in Figure 5.2.

5.2 Infinite-time LQR control

A FCS is often required to performed for periods of time much longer than time scales in the optimal gains. In this case we can assume that it is $t_f \to \infty$, which significantly simplifies the control design. In general, this situation is called the *infinite horizon*

problem. In this case, the cost function becomes,

$$J(\mathbf{x}(t), \mathbf{u}(t)) = \frac{1}{2} \int_0^\infty \left[\mathbf{x}^\top \mathbf{Q} \mathbf{x} + \mathbf{u}^\top \mathbf{R} \mathbf{u} \right] dt. \tag{5.8}$$

Since our concern is now the long-term steady-state response of the system, the problem of identifying the optimal gains becomes time independent and it can be assumed $\dot{\mathbf{P}} = 0$. Eq. (5.6) becomes

$$\mathbf{P}\mathbf{A} + \mathbf{A}^\top \mathbf{P} - \mathbf{P}\mathbf{B}\mathbf{R}^{-1}\mathbf{B}^\top \mathbf{P} = -\mathbf{Q}. \tag{5.9}$$

This equation is known as the *algebraic Riccati equation*. Eq. (5.7) now defines a constant feedback gain matrix,

$$\mathbf{K} = -\mathbf{R}^{-1}\mathbf{B}^\top \mathbf{P}. \tag{5.10}$$

An infinite-time LQR typically increases the stability of the system and the controller is then added as an inner loop to the pilot commands, with matrix $\mathbf{K}$ in Eq. (5.10) defining the constant feedback gain. This is referred to as the *stability augmentation system* (SAS). Other feedback systems are often also introduced to improve the responsiveness of the aircraft to the pilot inputs, and in that case it is said that they provide *command augmentation*. The control laws include multiple gains that are fine-tuned by the test pilots in flight test campaigns to achieve desired handling qualities.

5.2.1 An analytical example

Consider the following linear time-invariant system

$$\dot{\mathbf{x}}(t) = \mathbf{A}\mathbf{x} + \mathbf{B}u(t), \tag{5.11}$$

with

$$\mathbf{A} = \begin{bmatrix} -1 & 0 \\ 1 & 0 \end{bmatrix} \quad \text{and} \quad \mathbf{B} = \begin{bmatrix} 1 \\ 0 \end{bmatrix} \tag{5.12}$$

Let the states be here x_1 and x_2. An equation of this form appeared in eq. (4.30) as a simplified model for the lateral dynamics. There x_1 is the roll rate, x_2 is the roll angle, and u an antisymmetric aileron deflection. The cost function will be chosen as

$$J = \int_0^\infty \left(x_2^2 + Ru^2 \right) dt, \tag{5.13}$$

with $R > 0$, which penalizes the second state in the system (the roll angle) and the effort on the aileron, with a relative weight between the two given by R (e.g., if $R = 1$ they have equal weight). Given a value of R, the optimal gains for the closed-loop problem are obtained from the algebraic Riccati equation, eq. (5.9), which results here in the matrix

equation

$$\begin{bmatrix} P_{11} & P_{12} \\ P_{12} & P_{22} \end{bmatrix} \begin{bmatrix} -1 & 0 \\ 1 & 0 \end{bmatrix} + \begin{bmatrix} -1 & 1 \\ 0 & 0 \end{bmatrix} \begin{bmatrix} P_{11} & P_{12} \\ P_{12} & P_{22} \end{bmatrix} \\ -\frac{1}{R} \begin{bmatrix} P_{11} & P_{12} \\ P_{12} & P_{22} \end{bmatrix} \begin{bmatrix} 1 \\ 0 \end{bmatrix} \begin{bmatrix} 1 & 0 \end{bmatrix} \begin{bmatrix} P_{11} & P_{12} \\ P_{12} & P_{22} \end{bmatrix} = - \begin{bmatrix} 0 & 0 \\ 0 & 1 \end{bmatrix} \tag{5.14}$$

where we have used that the unknown matrix P is symmetric. It simplifies to

$$\begin{bmatrix} P_{11} & P_{12} \\ P_{12} & P_{22} \end{bmatrix} \begin{bmatrix} -R & 0 \\ R & 0 \end{bmatrix} + \begin{bmatrix} -R & R \\ 0 & 0 \end{bmatrix} \begin{bmatrix} P_{11} & P_{12} \\ P_{12} & P_{22} \end{bmatrix} - \begin{bmatrix} P_{11}^2 & P_{11}P_{12} \\ P_{11}P_{12} & P_{12}^2 \end{bmatrix} = \begin{bmatrix} 0 & 0 \\ 0 & -R \end{bmatrix} \tag{5.15}$$

The unknowns are therefore P_{11}, P_{12}, and P_{22} and their corresponding three (quadratic) equations are

$$\begin{aligned} -2RP_{11} + 2RP_{12} - P_{11}^2 &= 0, \\ -RP_{12} + RP_{22} - P_{11}P_{22} &= 0, \\ P_{12}^2 &= R. \end{aligned} \tag{5.16}$$

From the last equation it is $P_{12} = \sqrt{R}$. Then the first equation results in a second-order polynomial in P_{11} with roots, $P_{11} = -R \pm \sqrt{R^2 + 2R\sqrt{R}}$. Since $\mathbf{P}$ must be positive definite, then only the positive root is considered, which gives $P_{11} = -R + R\sqrt{1 + 2/\sqrt{R}}$ (positive for all $R > 0$). Finally, substituting this result into the second equation gives $P_{22} = \sqrt{R}/\sqrt{1 + 2\sqrt{R}}$. The optimal feedback gains are then given by eq. (5.10), which results in

$$\mathbf{K} = \frac{-1}{R} \begin{bmatrix} 1 & 0 \end{bmatrix} \begin{bmatrix} P_{11} & P_{12} \\ P_{12} & P_{22} \end{bmatrix} = \begin{bmatrix} 1 - \sqrt{1 + 2/\sqrt{R}} & -2/\sqrt{R} \end{bmatrix} \tag{5.17}$$

We can now close the loop as in fig. 5.2. The closed-loop system dynamics is obtained from replacing $u = \mathbf{K}\mathbf{x}$ in the state equation, that is,

$$\dot{\mathbf{x}} = \mathbf{A}\mathbf{x} + \mathbf{B}\mathbf{K}\mathbf{x} = (\mathbf{A} + \mathbf{B}\mathbf{K})\,\mathbf{x}. \tag{5.18}$$

By varying the control penalty R we can then explore its effect on the eigenvalues of the closed-loop system. First of all, we can compute the open-loop eigenvalues of the system (the eigenvalues of $\mathbf{A}$), which are $\lambda_1 = 0$ and $\lambda_2 = -1$. Note that, from eq. (5.17), when $R \to \infty$ it is $\mathbf{K} = \mathbf{0}$: the closed-loop system behaves as the open-loop system. This is because a very large penalty on the control u prevents it from acting outright. On the other extreme, the gains on the feedback matrix go to infinity as $R \to 0$, which means that if the penalty on the control is too small we have very large (non-physical)

actuation. Figure 5.3 shows the eigenvalues of the closed-loop for values of R ranging from 10^{-2} (where the system has two highly-damped complex pairs) to 10^4 (where the roots are very closed to those in open loop). A logarithmic distribution of R is used in that range.

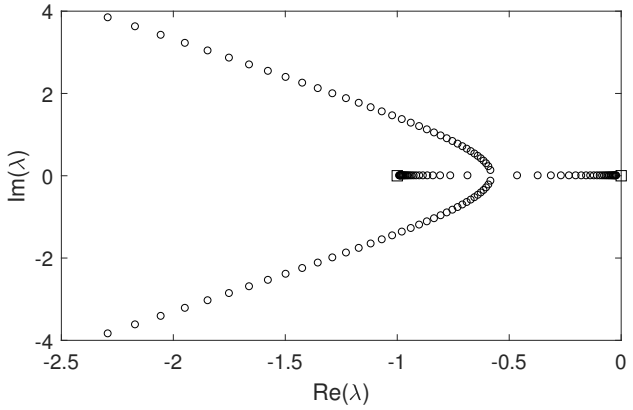

Figure 5.3: Closed-loop eigenvalues for $10^{-2} < R < 10^4$. The squares are the open-loop eigenvalues.

5.2.2 Numerical example: command tracking of a rigid aircraft

The linearized model for the lateral/directional dynamics is written as

$$\dot{\mathbf{x}}_d = \mathbf{A}_d\mathbf{x}_d + \mathbf{B}_d\mathbf{u}_d$$

with state vector $\mathbf{x}_d = \begin{Bmatrix}\beta & \phi & \omega_x & \omega_z\end{Bmatrix}^\top$, that is, sideslip and roll angles (in degrees), and roll and yaw rates (in deg/s), respectively, and with input vector $\mathbf{u}_d = \begin{Bmatrix}\delta_a & \delta_r\end{Bmatrix}^\top$, that is, deflections on ailerons and rudder (also in degrees). For an F-16, nominal configuration at 550 km/h, the state and input matrices are given in Stevens and Lewis (2003):

$$\mathbf{A}_d = \begin{bmatrix} -0.0322 & 0.064 & 0.0364 & -0.9917 \\ 0 & 0 & 1 & 0.0037 \\ -30.6492 & 0 & -3.6784 & 0.6646 \\ 8.5396 & 0 & -0.0254 & -0.4764 \end{bmatrix} \text{ and } \mathbf{B}_d = \begin{bmatrix} -0.0003 & -0.0008 \\ 0 & 0 \\ 0.7333 & -0.1315 \\ 0.0319 & 0.0620 \end{bmatrix}$$

The eigenvalues of the state matrix are $\lambda_1 = -0.42 \pm 3.06j$ (dutch roll),$\lambda_2 = -3.62$ (roll subsidence) and $\lambda_3 = -0.016$ (spiral). The corresponding eigenvectors are

	$\mathbf{x}_{d,1}$	$\mathbf{x}_{d,2}$	$\mathbf{x}_{d,3}$
β	$-0.10 \mp 0.08j$	0.00	0.00
ϕ	$-0.04 \mp 0.28j$	-0.27	1.00
ω_x	$0.88 \pm 0.00j$	0.96	-0.02
ω_x	$-0.23 \pm 0.28j$	0.01	0.06

The impulse response for 20 s is:

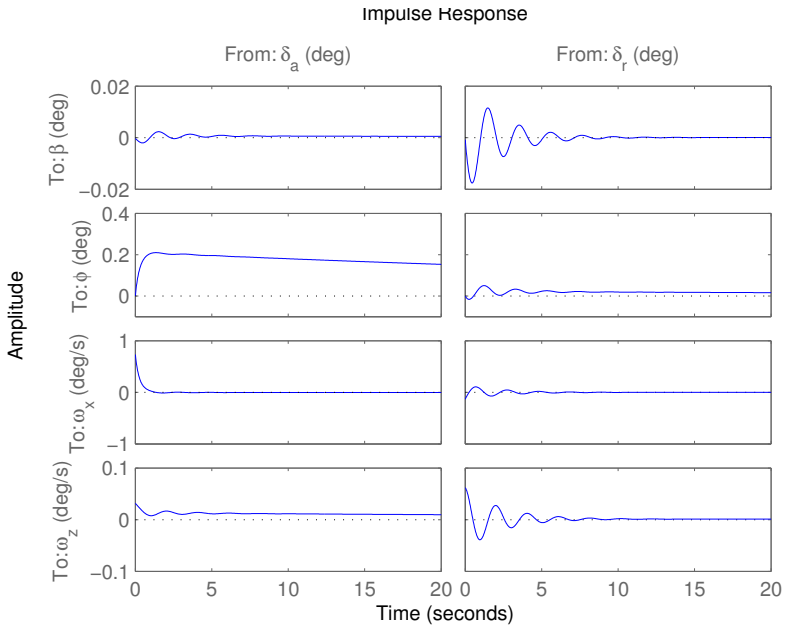

Results on the right show the impulse response to aileron excitation. The roll rate goes quickly back to zero, but the low damping on the spiral mode dominates the long-term response. Results on the right show the impulse response to rudder excitation, which is dominated by the low-damped dutch roll.

An infinite-time LQR is now sought. We choose Q and R to be diagonal. Since only the relative values between Q and R are relevant, the control weights can be first chosen. We give equal weights to aileron and rudder,

$$\mathbf{R} = \begin{bmatrix} 1 & 0 \\ 0 & 1 \end{bmatrix} \tag{5.19}$$

Then, for the $\mathbf{Q}$ matrix we give equal weights to the terms associated to yaw motions ($Q_{11} = Q_{44}$) and roll motions ($Q_{22} = Q_{33}$). We consider three cases:

Q_{11}	Q_{22}	λ_1	λ_2	λ_3
0	0	$-0.42 \pm 3.06j$	-3.62	-0.02
10	0	$-0.44 \pm 3.06j$	-3.62	-0.04
0	10	$-0.47 \pm 3.07j$	-4.28	-0.56
100	10	$-0.57 \pm 3.06j$	-4.29	-0.57

Q_{22} affects all modes, while Q_{11}, which is linked to the yaw motions, almost only affects dutch-roll. This is in agreement with the components of the eigenvectors identified above. The limit of how big the weights can be is established by how much we can deflect the control surfaces. In a problem with initial conditions such as the impulse response considered here, however, control surfaces will only reach saturation if the initial conditions are exceedingly large. Finally, for $Q_{11} = 100$ and $Q_{22} = 10$, the closed-loop response to impulse excitation on each of the control surfaces is:

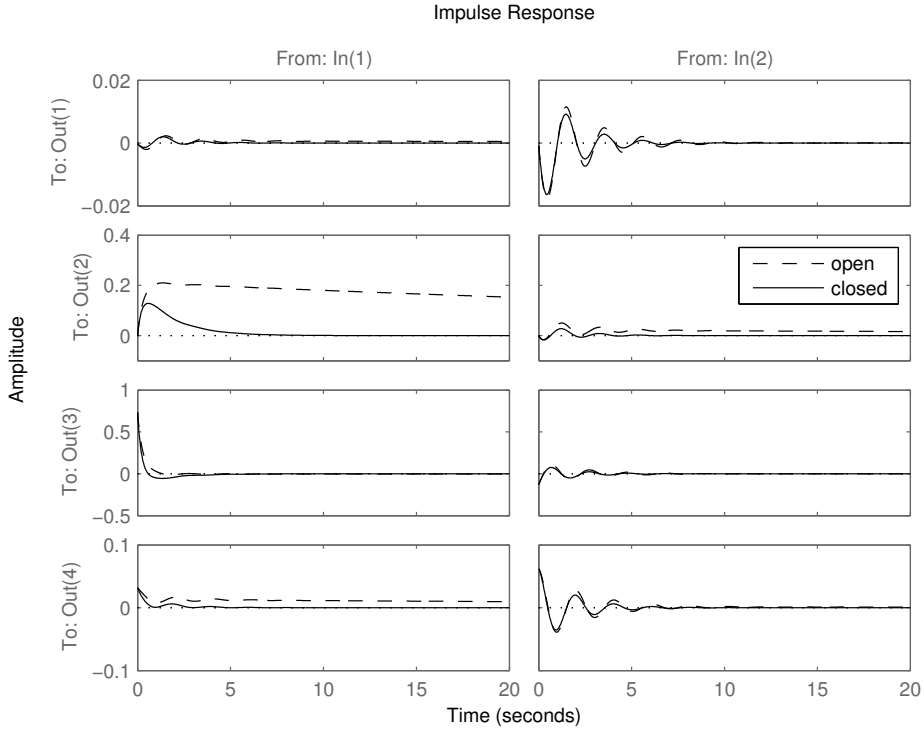

The corresponding time-history of the aileron inputs in the closed-loop response is:

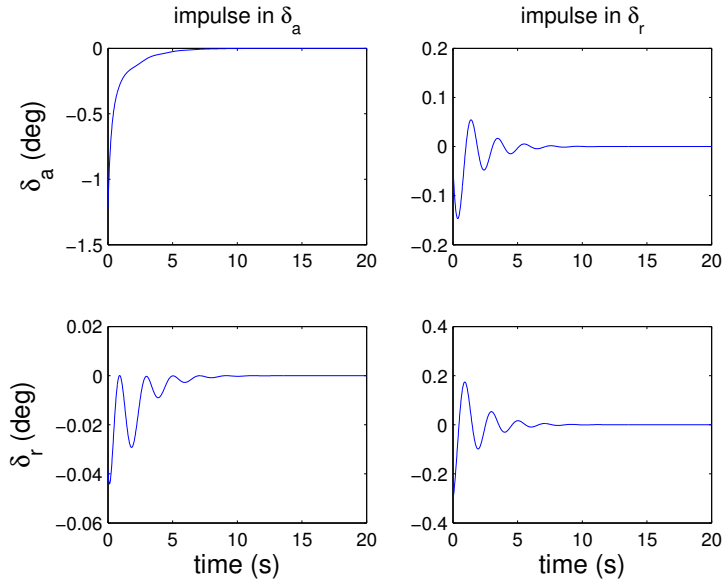

5.3 Further reading

Kirk (1970) and Burl (1999) provide good general introductions to optimal control methods. For aircraft applications, most recent textbooks on flight dynamics include descriptions of the key elements of a modern flight control system (Cook, 2013; Schmidt, 2012).

Bibliography

H. H. Ashley. *Engineering Analysis of Flight Vehicles*. Addison-Wesley Aerospace Series. Addison-Wesley Publishing Co., Reading, Massachussetts, USA, 1974.

J. B. Burl. *Linear Optimal Control – $\mathcal{H}_2$ and $\mathcal{H}_\infty$ Methods*. Addison-Wesley, Menlo Park, California, USA, 1999.

M. V. Cook. *Flight Dynamics Principles: A Linear Systems Approach to Aircraft Stability and Control*. Butterworth-Heinemann, 3rd edition, 2013.

A. Filippone. *Advanced Aircraft Flight Performance*. Cambridge University Press, New York, NY, USA, 2012.

D. E. Kirk. *Optimal Control Theory*. Prentice-Hall, Inc., Englewood Cliffs, New Jersey, USA, 1970.

R. C. Nelson. *Flight Stability and Automatic Control*. McGraw-Hill, Boston, Massachusetts, USA, 2nd edition, 1998.

M. C. Y. Niu. *Airframe Structural Design: Practical Design Information*. Hong Kong Conmilit Press, 2nd edition, 1999.

D. K. Schmidt. *Modern Flight Dynamics*. Mc-Graw Hill, New York, NY, USA, International edition, 2012.

R. F. Stengel. *Flight Dynamics*. Princeton University Press, 2004.

B. L. Stevens and F. L. Lewis. *Aircraft Control and Simulation*. John Wiley & Sons, Inc., 2nd edition, 2003.

J. R. Wright and J. E. Cooper. *Introduction to Aircraft Aeroelasticity and Loads*. John Wiley & Sons Ltd, 2007.

J. Xu and I. Kroo. Aircraft design with active load alleviation and natural laminar flow. *Journal of Aircraft*, 51(5):1532–1545, September–October 2014. doi: 10.2514/1.C032402.